CONSTITUTIVE MODELING AND COMPUTER METHODS IN GEOTECHNICAL ENGINEERING

CHANDRAKANT S. DESAI

About the author

Chandrakant S. Desai
The University of Arizona,
Department of Civil Engineering and Engineering Mechanics
Tucson, Arizona. USA
E-mail: csdesai@email.arizona.edu

Abstract

Computer methods are in the forefront of the procedures for analysis and design for geotechnical problems. Constitutive models that characterize the behavior of geologic materials and interfaces/joints play a vital role in the solutions obtained by using computer methods or any other solution procedure. The literature on both constitutive and computer models is wide; attention in this paper is devoted to the disturbed state concept (DSC) for constitutive modeling and the finite element method for computer solutions. The disturbed state concept, a unified and hierarchical approach, provides a unified framework for characterization of the behavior of geologic materials and interfaces/joints. Important factors such as elastic, plastic and creep responses, stress paths, volume change (contraction and dilation), disturbance (softening and damage or stiffening), thermal effects, partial saturation and liquefaction can be included in the same DSC framework. Because of its hierarchical nature, simplified models for specific applications can be derived from the DSC. It has been applied successfully for defining behavior of many geologic materials and interfaces/joints.

Procedures for the determination of parameters for the DSC models based on laboratory tests have been developed. Various models from the DSC have been validated at the specimen level with respect to laboratory test data. They have been validated at the practical boundary value problem level by comparing observed behavior in the field and/or simulated problems in the laboratory with predictions using computer (finite element) procedures in which DSC has been implemented; these have been presented in various publications by Desai and coworkers, and are listed in the References. Three typical examples of such validations at the practical problem level are included in this paper. It is believed that the DSC can provide unified and powerful models for a wide range of geomechanical and other engineering materials, and interfaces/joints.

Keywords

constitutive modeling, disturbed state concept – DSC, geologic materials, interfaces/joints

Dedication

Professor Lujo Šuklje was the pioneer of Slovenian Soil Mechanics, whose contributions were recognized internationally. He has made outstanding contributions in rheological properties of soils including creep and anisotropy, viscoplastic models, consolidation and foundation engineering. His book, Rheological Aspects of Soil Mechanics published in 1969, has left an indelible mark on the literature in engineering. I dedicate, with profound respects, this paper to the memory of Professor Šuklje.

1 INTRODUCTION

In the continuing pursuits for realistic models for geologic materials and interfaces or joints, a great number of simple, and simplified to complex constitutive models have been proposed. It is not the intention here to present a detailed review of such models, which includes elasticity, plasticity, creep, damage, micromechanics, micro-cracking leading to fracture and failure, and liquefaction. Such reviews are available in many publications, including Desai (2001b).

1.1 SCOPE

The modeling approach based on the disturbed state concept (DSC) is the main objective in this paper. The DSC provides a hierarchical and unified framework to include other models such as elasticity, conventional

plasticity, continuous hardening plasticity, creep, and micro-cracking leading to softening as special cases. Also, the number of parameters required in various versions of the DSC model is smaller or equal to the number in other available models of similar capabilities.

The DSC model has been implemented in two- and three-dimensional problems for dry and saturated geologic materials under static and cyclic (dynamic) loadings. Since the DSC model results in a special form of nonsymmetrical matrix equations, it is necessary to develop special schemes for the implementation of the DSC models in computer (finite element) procedures.

The descriptions of the DSC model and the finite element procedure are divided in the following components:

- Basic concept and hierarchical framework.
- Parameter determination and calibration from laboratory and/or field tests.
- Brief description of a special scheme for implementation of the DSC in the finite element procedure.
- Validations with respect to tests used for calibration and independent tests, and applications of the finite element method for solutions of a number of practical problems in geotechnical engineering.

2 BASIC CONCEPT AND HIERARCHICAL FRAMEWORK

Details of the DSC are given in various publications (e.g. Desai 1974, Desai 1987, Desai and Ma 1996, Desai and Toth 199, Katti and Desai 1995, Park and Desai 2000), which are referenced in Desai (2001b). A brief description of the framework is given below with attention to the calibration for DSC parameters, numerical implementation and validations.

2.1 EQUATIONS

The DSC is based on the idea that the observed behavior of a material can be expressed through the behavior of reference components in the deforming material. The reference components are usually called relative intact (RI) and fully adjusted (FA). The behavior of the RI part, which may not be affected by microstructural discontinuities, can be defined by using a continuum model, e.g. elasticity, plasticity or viscoplasticity. The RI part is transformed continuously to the FA part, distributed at random locations, Fig. 1. The RI and FA parts are coupled and interact to yield the observed response, which is expressed in terms of the RI and FA

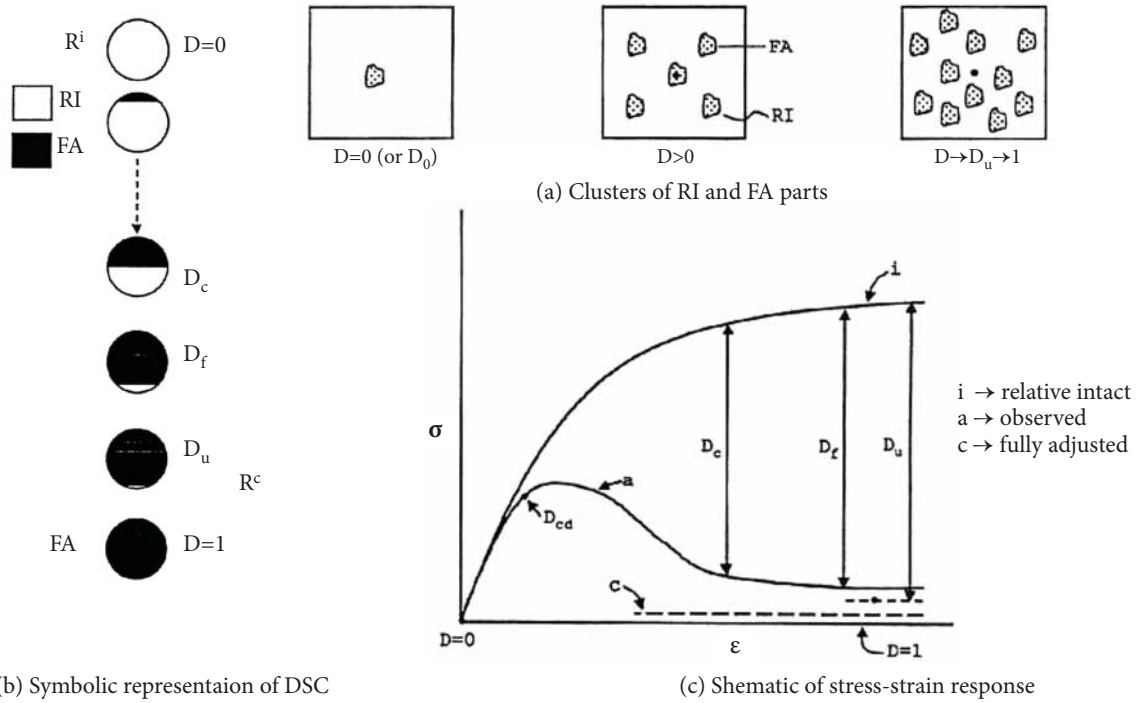

Figure 1. Representations of DSC.

behavior, connected through the disturbance function, which provides for the coupling. Based on the above concept, the incremental constitutive equations for DSC are derived as

$$d\underset{\sim}{\sigma}^{a} = (1-D)\ \underset{\sim}{C}^{i}\, d\underset{\sim}{\varepsilon}^{i} + D\underset{\sim}{C}^{c}\, d\underset{\sim}{\varepsilon}^{c} + dD\left(\underset{\sim}{\sigma}^{c} - \underset{\sim}{\sigma}^{i}\right) \qquad (1a)$$

or

$$d\underset{\sim}{\sigma}^{a} = \underset{\sim}{C}^{DSC}\, d\underset{\sim}{\varepsilon}^{i} \qquad (1b)$$

where σ = stress vector, ε = strain vector, *a*, *i* and *c* denote observed, RI and FA behavior, respectively, C^i and C^c = constitutive matrices for the RI and FA parts, respectively, D = disturbance and d denotes increment.

The RI behavior can be expressed by using a suitable continuum model, e.g., linear elastic, nonlinear elastic, elastic-plastic or viscoplasticity. Here, the hierarchical single surface (HISS) plasticity (associative) model (δ_0), derived from the general basis (Desai 1980), is used in which the yield function, F (Desai et al. 1986), is given by

$$F = J_{2D} - \left(-\alpha\, \bar{J}_1^{n} + \gamma\, \bar{J}_1^{2}\right)\left(1\text{-}\beta\, S_r\right)^{-0.50} = 0 \qquad (2)$$

where J_{2D} = second invariant of the deviatoric stress tensor, $\bar{J}_1 = J_1 + 3R$, J_1 = first invariant of the stress tensor, R = parameter related to the cohesive strength, $\bar{c}$, Fig. 2, γ = parameter related to the ultimate yield surface, β = parameter related to the shape of F in $\sigma_1 - \sigma_2 - \sigma_3$ stress space, S_r = stress ratio = $\left(\sqrt{27}/2\right)\left(J_{3D}/J_{2,3}^{3/2}\right)$, J_{3D}= third invariant of the deviatoric stress tensor, and α is the growth or hardening function. In Eq. (2), the stress invariants are nondimensionalized with respect to p_a, the atmospheric pressure constant.

In a simple form, the growth or hardening function is given by

$$\alpha = \frac{a_1}{\xi^{n_1}} \qquad (3a)$$

where a_1 and η_1 = hardening parameters and ξ is the trajectory of or accumulated plastic strains:

$$\xi = \int \left(d\varepsilon_{ij}^{p} \cdot d\varepsilon_{ij}^{p}\right)^{1/2} \qquad (3b)$$

in which ε_{ij}^{p} = plastic strain tensor, which is the sum of the deviatoric and volumetric plastic strains.

The FA part can be defined by assuming that it has no strength like in classical damage model (Kachanov 1986), or it has hydrostatic strength like in classical plasticity, or it has strength corresponding to the critical state model. It can be also defined by using the behavior of other states such as zero suction for partially saturated soils. For soils, it is found appropriate to use the critical state equations to define the FA response (Roscoe, et al. 1958, Desai 2001b):

$$\sqrt{J_{2D}^{c}} = \bar{m}\, J_1^{c} \qquad (4a)$$

$$e^{c} = e_o^{c} - \lambda\, \ell n \left(\frac{J_1^{c}}{p_a}\right) \qquad (4b)$$

where *c* denotes the critical state, *e* = void ratio, e_o^c = initial void ratio and $\bar{m}$, and λ are the critical state parameters.

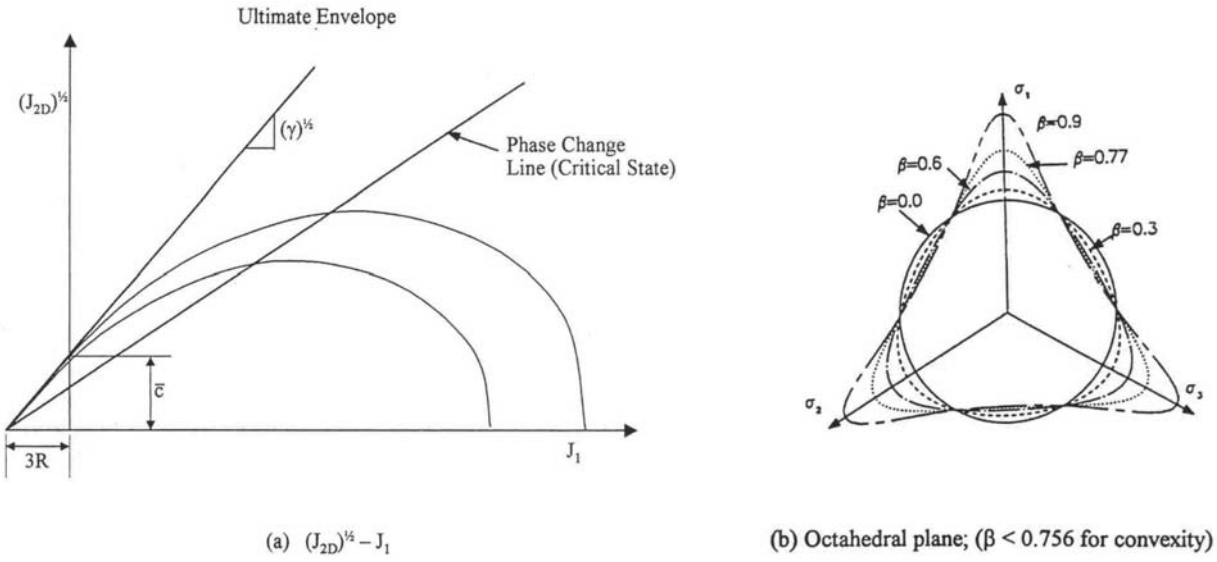

(a) $(J_{2D})^{1/2} - J_1$ (b) Octahedral plane; (β < 0.756 for convexity)

Figure 2. Plots of F in different stress spaces.

2.2 DISTURBANCE FUNCTION

The disturbance function, D, can be defined on the basis of observed stresses, volumetric strains, pore water pressures or nondestructive properties such as S- and P-wave velocities. In terms of stress, D is expressed as

$$D = \frac{\sigma^i - \sigma^a}{\sigma^i - \sigma^c} \qquad (5a)$$

The disturbance, D, is also expressed as (Fig. 3)

$$D = D_u \left(1 - e^{-A\xi_D^Z}\right) \qquad (5b)$$

where D_u = ultimate disturbance, A and Z are disturbance parameters, and ξ_D is the trajectory of deviatoric plastic strains.

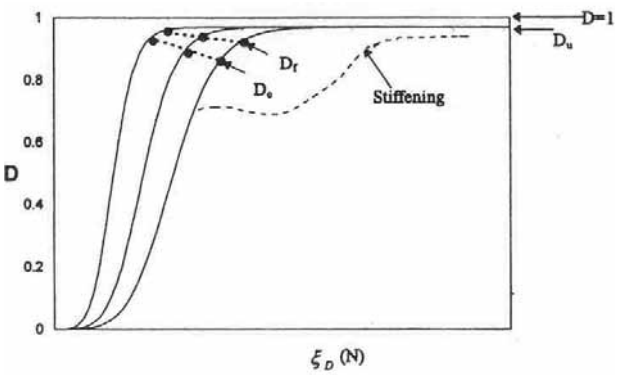

Figure 3. Disturbance for softening, stiffening behavior and critical disturbance.

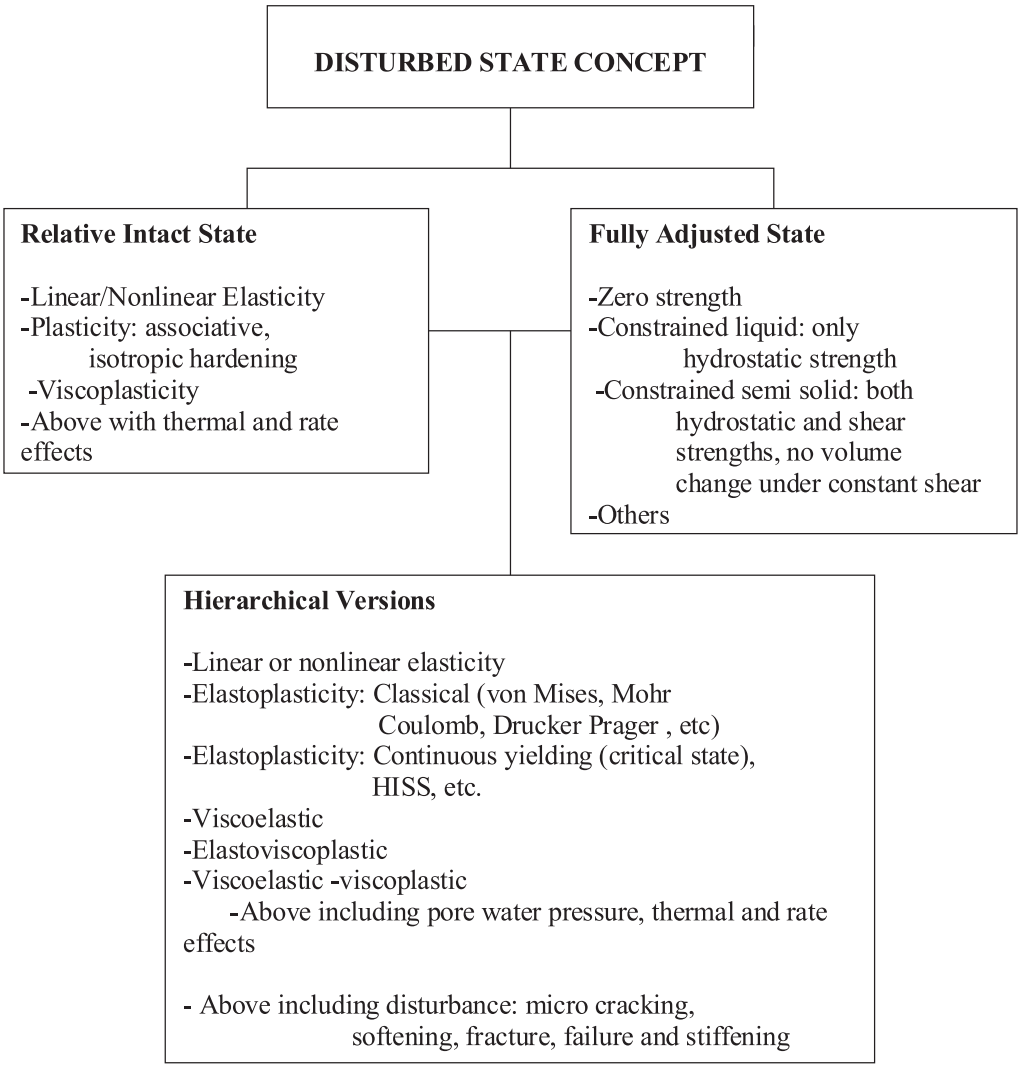

Figure 4. Hierarchical versions in DSC.

2.3 HIERARCHICAL APPROACH

Various continuum models can be derived from the DSC equations, Eq. (1). If $D = 0$, i.e., the material does not experience any microstructural changes leading to discontinuities, Eq. (1) reduce to that for standard continuum models:

$$d\ \underset{\sim}{\sigma}^i = \underset{\sim}{C}^i\ \mathrm{d}\,\underset{\sim}{\varepsilon}^i \qquad (6)$$

where C^i = constitutive matrix for continuum model, e.g., elasticity, plasticity, etc. Various models such as von Mises, Drucker-Prager, critical state, Matsuoka and Nakai (1974), Lade and Kim (1988), etc. can be obtained as special cases of the HISS model, Eq. (2). Fig. 4 shows various versions that can be derived from the DSC.

2.4 INTERFACE/JOINTS

Since both the solid material (soil) and the interfaces are coupled, it is appropriate to use the same mathematical framework for both. One of the major advantages of the DSC is that it provides the same framework for the solid material and the interfaces. It has been formulated for interface/joint behavior with suitable yield function for RI behavior and critical state models for FA behavior (Desai et al. 1984, Desai and Ma 1992, Desai et al. 1995, Desai 2001b, Desai et al. 2005). This paper essentially addresses the soil behavior.

2.5 ADVANTAGES OF DSC/HISS MODELS

The DSC allows for discontinuities experienced by a deforming material, that can often result in degradation or softening; it can also allow stiffening and healing in deforming materials. It is essential to include the existence and effect of discontinuous material in the model; then only can it provide consistent and improved characterization compared to other models based on continuum plasticity proposed and used to account for such behavior (Mroz et al. 1978), Pestana and Whittle 1999, Elgamal et al 2002).

Because the DSC allows for the coupling between the RI and FA responses, it can avoid such difficulties as spurious mesh dependence that occurs in classical damage models (Kachanov 1986). Also, if such a coupling is considered in the classical damage model by introducing additional enrichments (e.g. Bazant 1994, Mühlhaus 1995), the resulting models may be complex.

In the fracture mechanics approach, usually it is required to introduce cracks in *advance* of the loading. In contrast, the DSC does not need *a priori* introduction of cracks, and initiation and growth of micro-cracking, fracture and failure can be traced at appropriate locations depending upon the geometry, loading and boundary conditions, on the basis of critical disturbance, D_c, obtained from test results (Desai 2001b,Park and Desai 2000, Pradhan and Desai 2006).

The DSC allows identification of and initiation and growth of microstructural instability or liquefaction by using the critical disturbance (Desai et al. 1998, Desai 2000, Park and Desai 2000, Pradhan and Desai 2006).

The DSC/HISS models also possess the following advantages:

1. The yielding in the HISS model is assumed to be dependent on total plastic strains or plastic work. Hence, in contrast to other models such as critical state and cap in which yielding is based on the volumetric strains, the HISS model includes the effect of plastic shear strains also.
2. The yield surface allows for different strengths along different stress paths.
3. Because of the continuous and special shape of the yield surface, it allows for dilatational strains before the peak stress, which can be common in many geomaterials, Fig. 2(a), and later Fig. 7(b).
4. The DSC allows for degradation and softening, and it can allow also for stiffening or healing.
5. Introduction of disturbance can account for (a part) the nonassociative behavior, i.e., deviation of plastic strain increment from normality.
6. The DSC allows intrinsically the coupling between RI and FA parts and the nonlocal effects. Hence, it is not necessary to add extra or special enrichments, e.g., microcrack interaction, gradient and Cosserat schemes, etc. (Mühlhaus 1995).
7. The DSC is general and can be used for a wide range of materials: geologic, concrete, asphalt, ceramics, metal, alloys and silicon (Desai 2001b), if appropriate test data is available.
8. It can also be used for repetitive loading which may involve a large number of loading cycles; a procedure is described below.

2.6 REPETITIVE LOADING: ACCELERATED PROCEDURE

Computer analysis for 2- and 3-D idealizations for time dependent problems can be time consuming and expensive, especially when significantly greater number of cycles of loading need to be considered. Therefore, approximate and accelerated analysis procedures have been developed for a wide range of problems in civil

(pavements) (Huang 1993), mechanical engineering and electronic packaging (Desai and Whitenack 2001). Here, the computer analysis is performed for only a selected initial cycles (say, 10, 20), and then the growth of plastic strains is estimated on the basis of empirical relation between plastic strains and number of cycles, obtained from laboratory test data. A general procedure with some new factors has been developed and applied for analysis of pavements and chip-substrate systems in electronic packaging (Desai 2007; Desai and Whitenack 2001).

From experimental cyclic tests on engineering materials, the relation between plastic strains (in the case of DSC, the deviatoric plastic strain trajectory, ξ_D), and the number of loading cycles, N, can be expressed as, Fig. 5:

$$\xi_D(N) = \xi_D(N_r)\left(\frac{N}{N_r}\right)^b \qquad (7)$$

where N_r = reference cycle, and b is a parameter, depicted in Fig. 5. The disturbance equation (5b) can be written as

$$D = D_u\left[1-\exp\left(-A\left\{\xi_D(N)^Z\right\}\right]\right. \qquad (8)$$

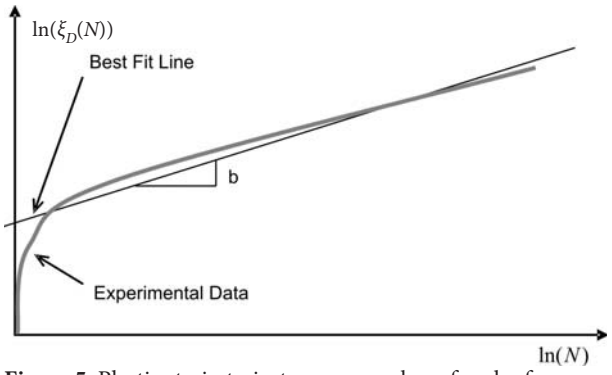

Figure 5. Plastic strain trajectory vs. number of cycles for approximate accelerated analysis.

Substitution of ($\xi_D(N)$) from Eq. (7) in Eq. (8) leads to

$$N = N_r\left[\frac{1}{\xi_D(N_r)}\left\{\frac{1}{A}\ell n\left(\frac{D_u}{D_u - D}\right)\right\}^{1/Z}\right]^{1/b} \qquad (9)$$

Now, Eq. (9) can be used to find the cycles to failure, N_f, for chosen critical value of disturbance = i (say, 0.50, 0.75, 0.80).

The accelerated approximate procedure for repetitive load is based on the assumption that during the repeated load applications, there is no inertia due to "dynamic" effects in loading. The inertia and time dependence can be analyzed by using the 3-D and 2-D procedures; however, for million cycles, it can be highly time consuming. Applications of repeated load in the approximate procedure involve the following steps:

1. Perform full 2-D or 3-D FE analysis for cycles up to N_r, and evaluate the values of $\xi_D(N_r)$ in all elements (or at Gauss points).
2. Using Eq. (7) compute $\xi_D(N)$ at selected cycles in all elements.
3. Compute disturbance in all elements using Eq. (8).
4. Compute cycles to failure N_f by using Eq. (9), for the chosen value of D_c.
5. The above value of disturbance allows plot of contours of D in the finite element mesh, and based on the adopted value of D_c, it is possible to evaluate extent of fracture and cycles to failure, N_f.

Loading-Unloading-Reloading: Special procedures and integrated in the codes to allow for loading, unloading and reloading during the repetitive loads; details are given in (Shao and Desai 2000, Desai 2001b).

3 PARAMETER DETERMINATION AND CALIBRATION FROM LABORATORY AND /OR FIELD TESTS

3.1 PARAMETERS

Based on the RI (Eq. 2), FA (Eq. 4) and disturbance, D (Eq. 5), the parameters required are:

Elastic	E and ν (or K and G)
RI: Plasticity	γ, β, n, a_1, η_1
FA: Critical state	e_0, m, λ
Disturbance	D_u, A and Z

where E = elastic modulus, ν = Poisson's ratio, K = bulk modulus, and G = shear modulus. The above parameters are averaged from the parameters obtained from test data under different confining pressures, and other facors. If the variation is severe, then a parameter needs to be expressed as a function of the factor, which increases the number of parameters. The number of parameters can increase if additional factors such as temperature and rate dependence are considered (Desai 2001b).

The following Table 1 gives some of the specialized versions with related number parameters. It may be noted that the number of parameters in the DSC model is less than or equal to those in any other available model of comparable capabilities.

Table 1. Specialized Versions and Parameters from DSC/HISS Model.

Specialization	Number of parameters
Elastic	2
Classical Elastic-plastic:	
- von Mises	3
- Mohr Coulomb	4
- Drucker-Prager	4
Continuous Hardening:	
- Critical State	5
HISS δ_0 Model (associative plasticity)	8*
HISS δ_1 Model (nonassociative plasticity)	9
HISS δ_{0+vp} Viscoplastic	11
HISS δ_2 Anisotropic	12
HISS δ_0 Disturbance	12

* If the cohesive strength is not included, the number of parameters reduces by 1.

Note: The number of parameters increases by about 2 if pore water pressure is considered and by about 2 if temperature is included.

3.2 PARAMETER DETERMINATION

The laboratory tests used for the calibration include consolidation (hydrostatic), triaxial and multiaxial and/or shear tests. The field test may include nondestructive, e.g., S-wave measurements. Direct shear and simple shear (e.g., using the CYMDOF device, Desai and Rigby, 1997) tests are used for DSC parameters for interfaces/joints (Desai 2001b).

The values of elastic moduli are found from the slopes of unloading responses. For instance, E is found from unloading slopes of $\sigma_1 - \sigma_3$ vs. ε_1 plots from triaxial tests. Similarly, ν can be found from plot of ε_v vs. ε_1 (ε_v = volumetric strain), G can be found from shear stress vs. shear strain plot, and K can be found from mean pressure (p) vs. ε_v plot. Determinations of various elastic parameters are depicted in Fig. 6.

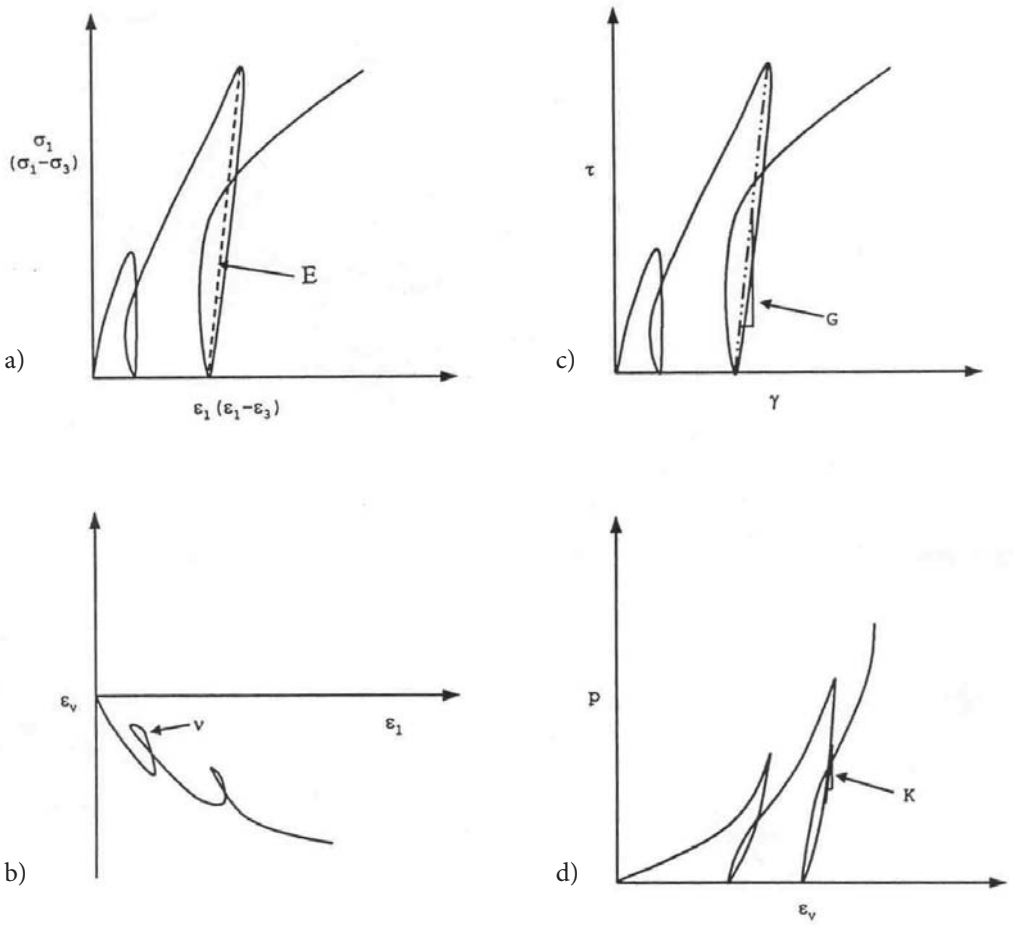

Figure 6. Elastic constants from test data; (a) stress-strain behavior, (b) volumetric-strain behavior, (c) shear stress-strain behavior, and (d) pressure -volumetric stain behavior.

The parameters γ and β are related to the *ultimate response*, which is often adopted from the asymptotic value (about 5 to 10% higher than the peak stress) for a given stress-strain curve, Fig. 7(a). They are found from the specialized expression for F (where $\alpha = 0$), Eq. (2), at the ultimate stress conditions, based on tests under different confining pressures:

$$F = J_{2D} - \gamma \, \overline{J}_1^2 \, \left(1\text{-}\beta \, S_r\right)^{-0.50} = 0 \qquad (10)$$

By substituting different values of ultimate stresses, Fig. 2, γ and β are found by using procedures such as the least-square method.

The phase change parameter is found from the point (b) in the stress-strain behavior, Fig. 7(b), where the response *transits from compressive to dilative*. One of the expressions for n is

$$n = \left. \frac{2}{1 - \left(\frac{J_{2D}}{J_1} \cdot \frac{1}{F_s \gamma} \right)} \right|_{d\varepsilon_v = 0} \qquad (11)$$

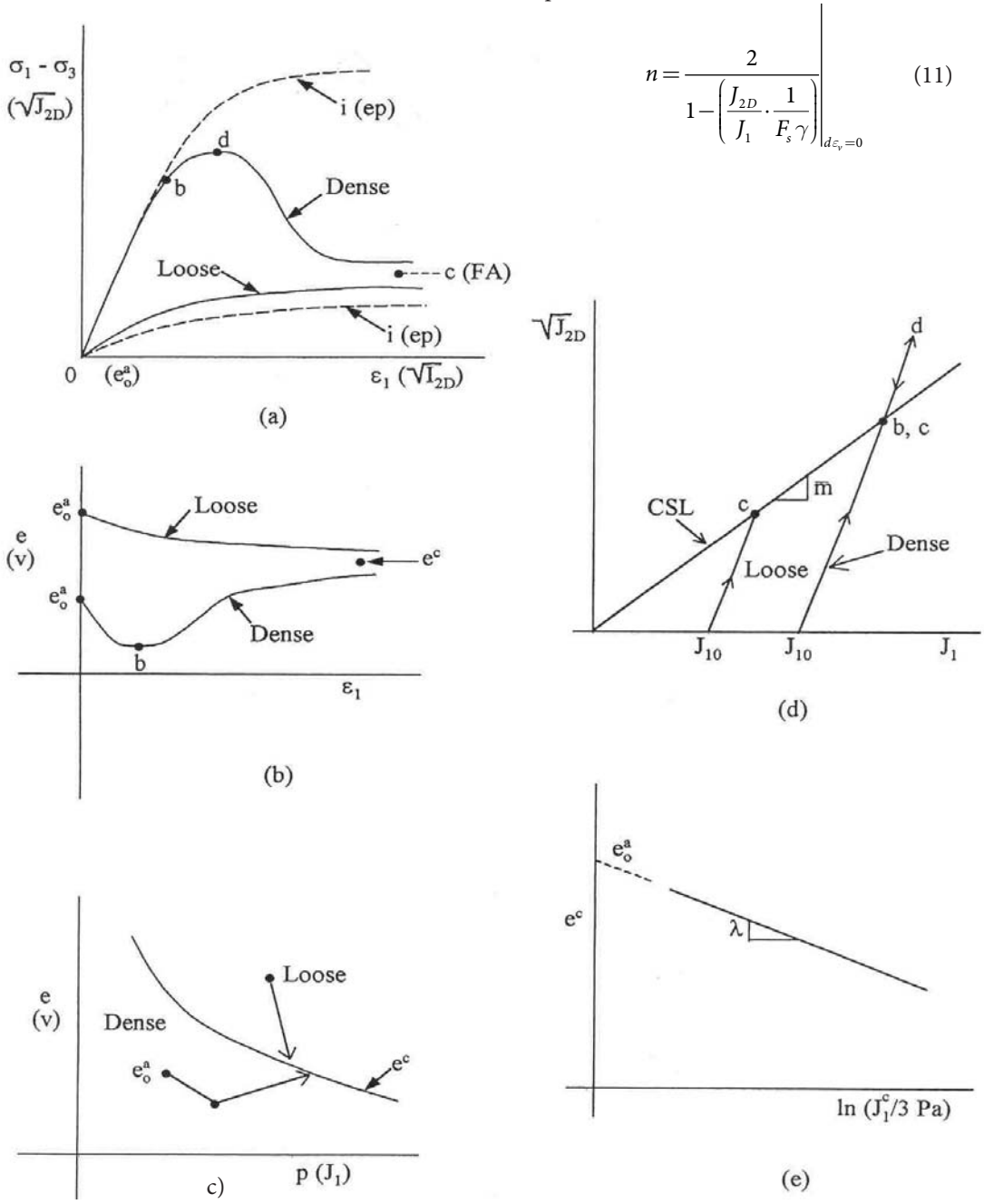

Figure 7. Behavior of loose and dense geo-materials: (a) stress-strain behavior, (b) volumetric–strain behavior, (c) void ratio-pressure behavior, (d) J1 - $\sqrt{J_{2D}}$ - critical state behavior, and (e) void ratio-critical state behavior.

The *hardening parameters* are determined based on the following expression from Eq. (3).

$$\ell n\alpha + \eta_1 \ell n\xi = \ell n\, a_1 \qquad (12)$$

Here, the stress-strain curve, Fig. 8(a) is divided into increments and ξ is found as the accumulated plastic strain for a given increment. Then α for a given ξ is found from Eq. (1), i.e., F = 0. The plot of (Fig. 8b) $ln\alpha$ vs. $ln\xi$ yield the (average) values of a_1 and η_1.

The critical state parameters, Eq. (4), are obtained from the plots of $\sqrt{J_{2D}} - J_1$ for $\bar{m}$ and e^c vs. $\ell n\left(J_1^c / p_a\right)$ for e_o^c and λ, Figs. 7(d) and 7(e).

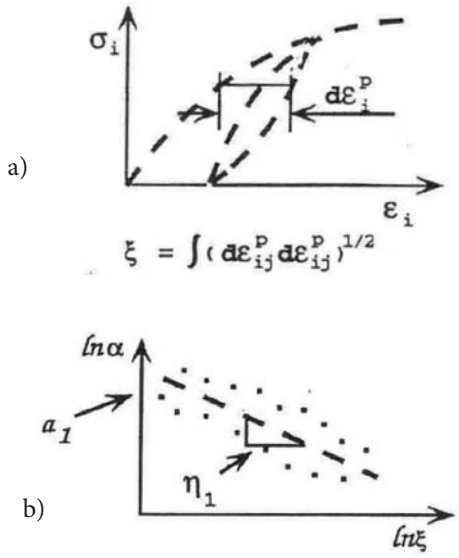

Figure 8. Determination of hardening or growth parameters, a_1 and η_1.

The disturbance parameter, D_u, is found from Eq. (5b) by substituting the value of the residual (FA) stress, Fig. 7(a). Then the values of A and Z are obtained by plotting $\ell n\left(-\ell n\left(D_u - D\right)/D_u\right)$ vs. $ln\xi_D$, Fig. 9, based on the following expression from Eq. (5):

$$Z\ell n\left(\xi_D\right) + \ell nA = \ell n\left[-\ell n\left(\frac{D_u - D}{D_u}\right)\right] \qquad (13)$$

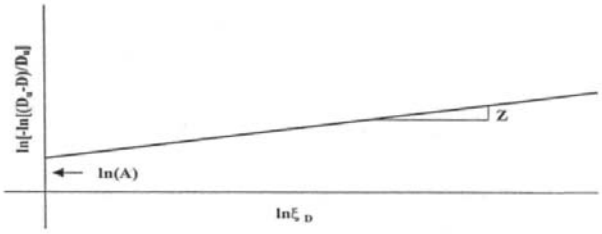

Figure 9. Determination of disturbance parameters, A and Z.

The values of D can be found from static or cyclic response, Fig. 1(c) or Fig. 10.

3.3 PARAMETERS FOR TYPICAL MATERIALS AND INTERFACES/JOINTS

The DSC models have been used to model a wide range of materials, e.g., clays, sands (dry and saturated), glacial tills, partially saturated soils, rocks, concrete, asphalt concrete, metals, alloys (solder), silicon., and various interfaces and joints. Application for interfaces includes clay-steel, sand-steel, sand-concrete and chip-substrate. Laboratory and/or field tests have been used to calibrate the DSC parameters by following the foregoing proce-

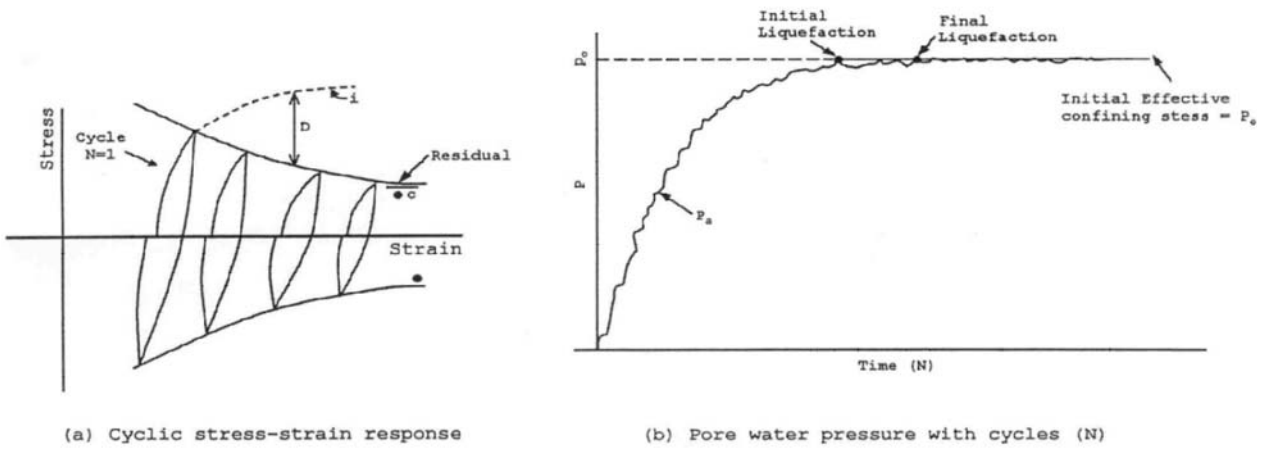

Figure 10. Cyclic tests for disturbance and liquefaction.

dures. Details of the parameters have been presented in a number of publications, and also given in Desai (2001b). Parameters for the relevant geologic materials and interfaces are given in the following Examples 1 to 3.

3.4 HIERARCHICAL VERSIONS

Various plasticity models such as nonassociative (δ_1) and anisotropic hardening (δ_2) can be obtained by modifying or adding "corrections" in the HISS model for the factors that influence the specific behavior, to the basic associative (δ_0) model (Desai et al. 1986, Somasundaram and Desai 1988, Wathugala and Desai 1993). Since the introduction of disturbance can account for (some) nonassociative response, the DSC model with the basis associative (δ_0) version is found to account for behavior of most geologic materials.

3.5 OTHER CAPABILITIES IN DSC

3.5.1 Creep Models

A schematic of the creep behavior is shown in Fig. 11. Various creep models, e.g., Maxwell, viscoelastic (ve), elastoviscoplastic (evp), and viscoelastic- viscoplastic (vevp), can be obtained as specialization of the Multicomponent DSC (MDSC) (Desai, 2001b). For example, the evp model can be defined based on the Perzyna's theory (1966), in which viscoplastic strain increment, $\dot{\varepsilon}^{vp}$, is expressed as

$$\dot{\varepsilon}^{vp} = \Gamma \langle \phi \rangle \frac{\partial F}{\partial \underset{\sim}{\sigma}} \qquad (14)$$

where Γ = fluidity parameter, and < > has the meaning of a switch-on-switch-off operator as

$$\left\langle \phi\left(\frac{F}{F_o}\right) \right\rangle = \begin{cases} \phi\left(\dfrac{F}{F_o}\right) & \text{if} \quad \dfrac{F}{F_o} > 0 \\ 0 & \text{if} \quad \dfrac{F}{F_o} \le 0 \end{cases} \qquad (15)$$

F_o = reference value of F (e.g., yield stress or p_a) and ϕ = flow function. One of the expressions of ϕ is

$$\phi = \left(\frac{F}{F_o}\right)^N \qquad (16)$$

In above equations, Γ and N are the viscous parameters. The values of Γ and N are found from a creep test, Fig. 11; details are given in (Desai et al. 1995, Desai 2001b). Various creep models such as viscoelastic (ve), viscoplastic (vp), viscoelastic -viscoplastic (vevp) can be obtained from the MDSC; they are depicted in Fig. 12. The Overlay or mechanical sub layer models (Duwez 1935, Zienkiewicz el al. 1972, Pande et al. 1977) can be considered to be special case of the MDSC approach.

3.5.2 Liquefaction

Liquefaction in saturated soils (Fig. 10) subjected to dynamic (or static) loading can be identified in the DSC by locating the critical value of the disturbance, D_c, Eq. (5), Fig. 3, that represents the microstructural instability. There is no additional parameter needed for liquefaction. Details of the development and use of the DSC for liquefaction are given in various publications (Desai et al. 1998b, Desai 2000, Park and Desai 2000, Pradhan and Desai 2006).

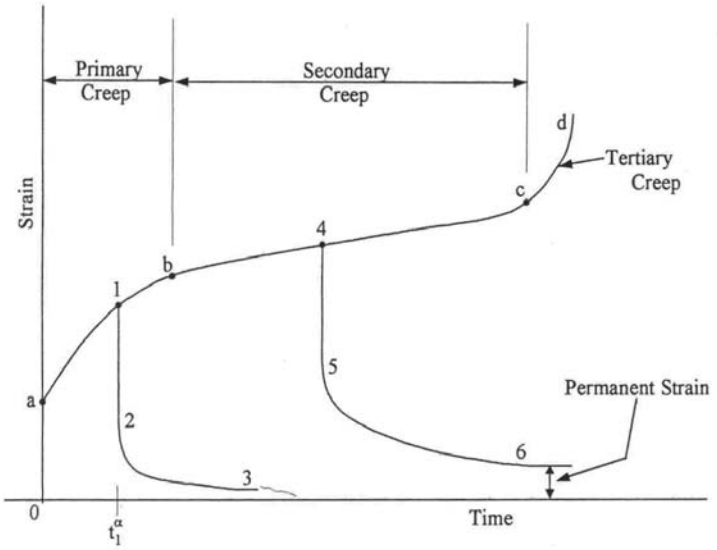

Figure 11. Schematic of creep behavior.

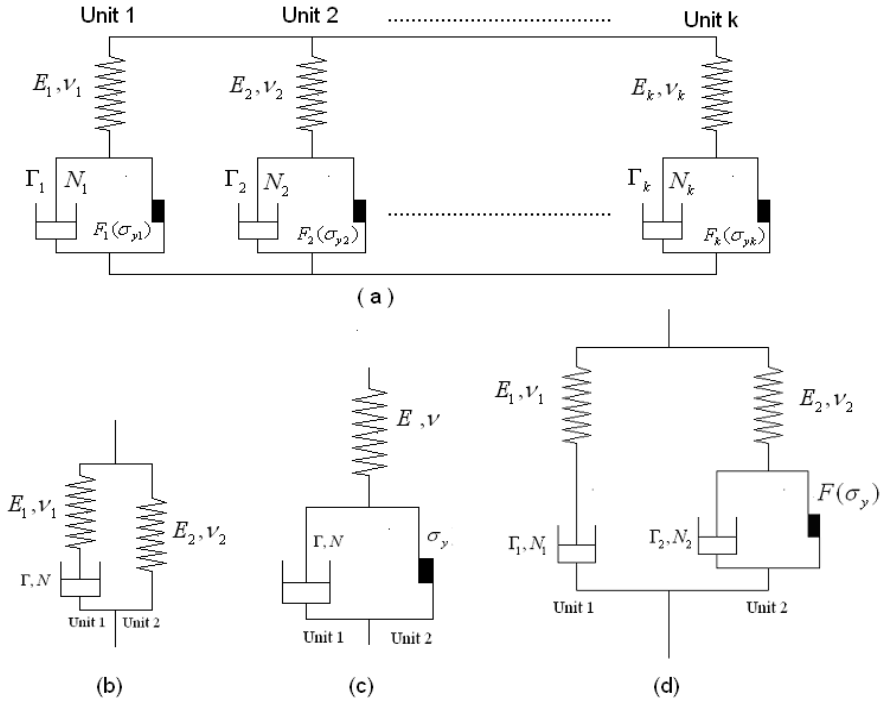

Figure 12. (a) MDSC creep models, (b) viscoelastic (ve), (c) viscoplastic (evp), and (d) viscoelastic-viscoplastic (vevp) models (Desai 2001b).

3.5.3 Partially saturated soils

The DSC model can be applied to model partially saturated soil by including factors such as suction and saturation (Geiser et al. 1997, Desai 2001b).

3.5.4 Stiffening and Healing

The disturbance, D, can simulate softening or degradation. It can also define stiffening or healing (Fig. 3) in the microstructure; for example, chemical and thermal (causing particle fusing) effects can increase in the bonding in the microstructure (Desai et al 1998a, Desai, 2001b).

3.5.5 Thermal Effects

The thermal effects can be introduced in the DSC model. Very often, the parameters are expressed as a function of temperature, T, as (Desai 2001b)

$$p = p_r \left(\frac{T}{T_r} \right)^c \qquad (17)$$

where p = any parameter, and p_r is the value of the parameters at a reference temperature, T_r (e.g., the room temperature), and c = parameter.

3.5.6 Rate Effects

Behavior of many materials is affected by the rate of loading. For a plasticity model, the rate effect can be introduced by modifying the static yield function determined from tests conducted under very slow or static rate (Baladi and Rohani 1984, Sane et al. 2009):

$$F_d = (F_s - F_R) / F_o \qquad (18)$$

where F_d represents the yield function defined for 'dynamic ' rate, F_s represents the yield function at static or very small rate, F_o is the used to nondimensionalize the terms, and F_R is the rate dependent function. Details for the determination F_R and F_s are given in (Sane et al. 2009).

3.6 COMMENTS ON VARIOUS ISSUES

3.6.1 Physical Meanings and Curve Fitting

A constitutive model for defining behavior of a material requires a certain level of curve fitting for calibration of parameters based on the test data. It is useful and desirable that such curve fitting is reduced as much as possible, particularly if the behavior is influenced by many factors. One of the ways is to develop parameters

that have physical meanings, e.g., the parameters are associated with physical states during the response, such as ultimate condition, and change in volumetric strain. Most of the parameters in the DSC have such physical meanings; hence, the need for curve fitting is reduced and the procedures for the determination of parameters are simplified.

3.6.2 simple and simplified models

It is often said that a constitutive model should be simple, particularly for practical applications. A functional representation (e.g., parabola, hyperbola, spline, etc.) of a given (single) stress-strain response as a nonlinear elastic model, is considered to be a "simple" model. Such a function like the hyperbola extended to include the effect of the confining pressure may still be called "simple". However, since the soil behavior is affected by other practical factors such as irreversible (plastic) deformations, stress path, volumetric strains, creep and type of loading, the resulting model may not be simple! It is apparent that models by using only mathematical functions (e.g. hyperbola, spline, etc) to represent stress-strain curves are not able to account for such practical factors.

Then, it is better to develop and use "simplified" models. A simplified model should be derived on the basis of basic principles of mechanics, and is intended to characterize the behavior affected by significant factors important for practical problems. It is often obtained by deleting less significant factors from a general model developed by considering the physical nature of the problem, loading and other relevant conditions. In other words, a "simplified" model could include the effect of the significant factors, in which the number of parameters could increase with the inclusion of each additional factor.

An important issue is how many parameters the model involves, and what type of tests are required to determine the parameters. The other important issue is how many significant factors are vital for practical problems and must be included in the model? It is natural that the number of parameters would increase with the number of factors. Hence, for a practical application, one must adopt a model that contains the influence of the significant factors for a particular application. Then the notion of adopting just a simple model that is not capable of accounting for practically important factors would have no basis!

Indeed, for practical applications, it is desirable to develop as simplified model as possible with smaller number of parameters. The DSC/HISS model has been developed such that its simplified versions can be adopted depending upon the need of the practical application. Moreover, the DSC/HISS model is hierarchical in nature and allows selection of a model for required factors by introducing additional factors and related parameters in the same basic model. The hierarchical approach in the DSCC/HISS model can reduce the number of parameters, and simplify the procedure for their determination based on standard (e.g., triaxial and shear) tests.

3.6.3 DSC and Damage models

The classical damage approach (Kachanov 1986) is based on the physical cracks (damage) in a deforming material, and the resulting effect on the observed behavior. The DSC is different from the damage approach in that it considers a deforming material as a mixture of two or more reference components (e.g., RI and FA states); then the observed behavior is expressed in terms of the behavior of the components, which interact to yield the observed behavior. The disturbance represents the deviation of the observed behavior from the reference state(s). Damage model can be considered as a special case of DSC if the interaction is removed, e.g., the FA state is assumed to possess no strength. However, such a model, without interaction between RI and FA states, may not be realistic and possesses certain (computational) difficulties (Desai 2001b). Moreover, the DSC approach is general and can include both softening and stiffening effects.

4 FINITE ELEMENT FORMULATION INCLUDING SPECIAL SCHEMES

The procedure for implementation of the DSC model in computer (finite element) methods is given below.

The finite element equations for two- or three-dimensional problems (Fig. 13) can be derived as (Desai, 2001b):

$$\int_V \underset{\sim}{B}^T \underset{\sim}{\sigma}^a_{n+1}\, dV = \underset{\sim}{Q}_{n+1} \qquad (19a)$$

where B = strain-displacement transformation matrix, $\underset{\sim}{\sigma}^a_{n+1}$ = observed stress vector at $n + 1$ step and the load vector:

$$\underset{\sim}{Q}_{n+1} = \int_V \underset{\sim}{N}^T \underset{\sim}{\overline{X}}\, dV + \int_{S_1} \underset{\sim}{N}^T \underset{\sim}{\overline{T}}\, dS' \qquad (19b)$$

where N = matrix of interpolation functions, $\underset{\sim}{\overline{X}}$ = body force vector, $\underset{\sim}{\overline{T}}$ = surface traction vector, V denotes volume and S_1 denotes a part of the surface.

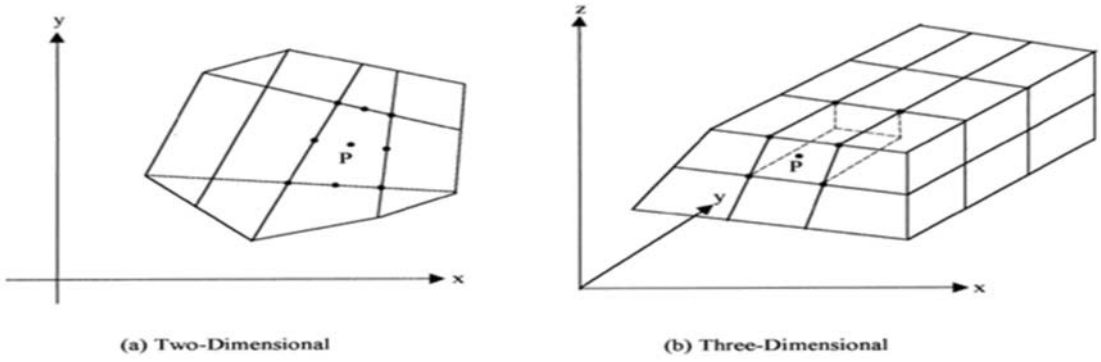

Figure 13. Finite Element Discretization: 2-D and 3-D elements.

Now with

$$\sigma^{a}_{n+1} = \sigma^{a}_{n} + d\sigma^{a}_{n+1} \qquad (20)$$

where n denotes increment, the incremental equations are:

$$\int_V \underset{\sim}{B}^T \, \mathrm{d}\underset{\sim}{\sigma}^{a}_{n+1} \, \mathrm{dV} = \underset{\sim}{Q}_{n+1} - \int_V \underset{\sim}{B}^T \underset{\sim}{\sigma}^{a}_{n} \, \mathrm{dV} = \underset{\sim}{Q}_{n+1} - \underset{\sim}{Q}^{b}_{n} = d\,\underset{\sim}{Q}^{b}_{n+1} \qquad (21)$$

where Q^b represents the internal balanced load at step n, Fig. 14, and $d\,Q^b$ denotes the out-of-balance or residual load vector.

Now, by substituting Eq. (20) in Eq. (19a), the incremental equations with the DSC model are:

$$\int_V \underset{\sim}{B}^T \underset{\sim}{C}^{DSC}_{n} \, \mathrm{B} \, \mathrm{dV} \cdot \mathrm{dq}^{\mathrm{i}}_{n+1} = d\mathrm{Q}^{\mathrm{b}}_{n+1} \qquad (22)$$

where $\underset{\sim}{C}^{DSC}_{n} = (1-D_n)\,\underset{\sim}{C}^{i}_{n} + \mathrm{D_n}\,(1+\alpha)\,\mathrm{C}^{\mathrm{c}}_{\mathrm{n}} + \underset{\sim}{\mathrm{R}}^T\,\sigma^{\mathrm{r}}_{\mathrm{n}}$; $\underset{\sim}{\sigma}^{r}_{n} = \underset{\sim}{\sigma}^{c}_{n} - \underset{\sim}{\sigma}^{i}_{n}$, $\mathrm{dD_n} = \underset{\sim}{R}^T\,\mathrm{d}\,\underset{\sim}{\varepsilon}^{i}_{n}$ (Desai, 2001b), and $d\,\underset{\sim}{\sigma}^{c}_{n} = (1+\alpha)\,\underset{\sim}{C}^{c}_{n}\,\mathrm{d}\,\underset{\sim}{\varepsilon}^{i}_{n}$ and α is the factor for relation between RI and FA strains.

Now, we can write Eq. (22) as

$$\underset{\sim}{k}^{DSC}_{n} \, \mathrm{dq}^{\mathrm{i}}_{n+1} = d\mathrm{Q}^{b}_{n+1} \qquad (23)$$

where $\underset{\sim}{k}^{DSC} = \int_V \underset{\sim}{B}^T \, \mathrm{C}^{DSC}_{n} \cdot \underset{\sim}{B} \cdot d\,\mathrm{V}$.

A number of procedures are possible for the solution of Eq. (23) (Desai, 2001b). Since k^{DSC}_{n} is nonsymmetrical, it may cause computational problems. Simplified and approximate procedure used commonly is briefly described below. This procedure is based on the solution of the RI behavior in which the stiffness matrix is symmetric:

$$\underset{\sim}{k}^{i}_{n} \, \mathrm{d}\,\underset{\sim}{q}^{i}_{n+1} = \mathrm{dQ}^{i}_{n+1} = \mathrm{Q}^{i}_{n+1} - \mathrm{Q}^{b(i)}_{n} \qquad (24)$$

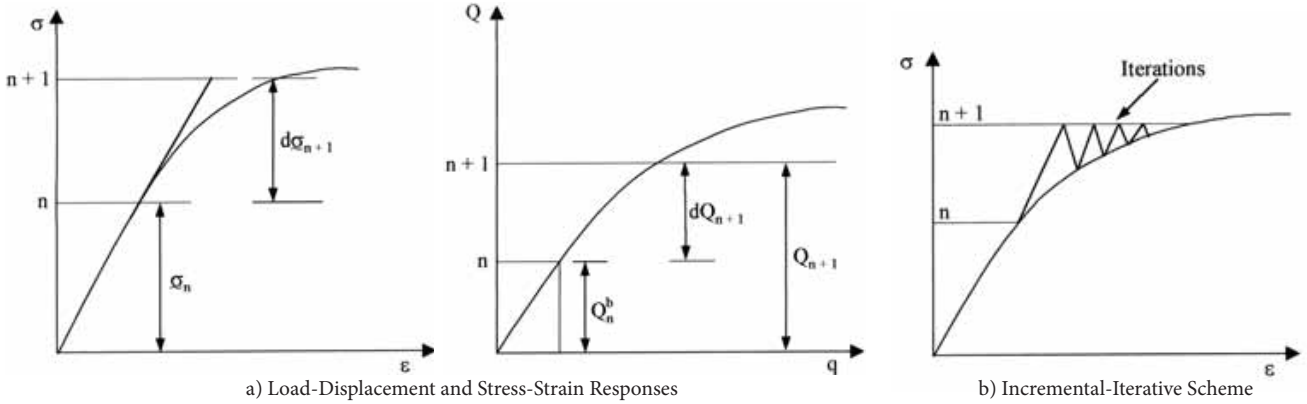

a) Load-Displacement and Stress-Strain Responses

b) Incremental-Iterative Scheme

Figure 14. Incremental iterative analysis.

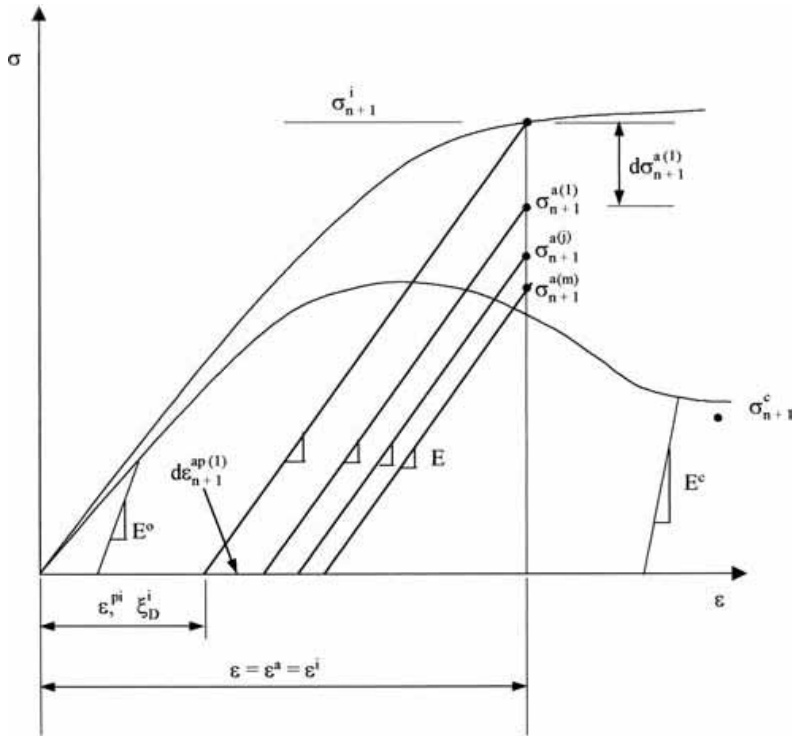

Figure 15. Iterative procedure in solution based on RI equations.

Fig. 15 shows the schematic of the procedure where the solution, Eq. (24) pertains to the continuously hardening (RI) behavior. Once the incremental displacements, $\mathrm{d}\ \mathrm{q}^{i}$, for the RI behavior are determined, the strains $\left(\mathrm{d}\ \underset{\sim n+1}{\overset{\sim n+1}{\varepsilon^{i}}}\right)$ and stresses $\left(\mathrm{d}\ \underset{\sim n+1}{\sigma^{i}}\right)$ are determined. Then the observed stresses are found from the following equation:

$$d\,\underset{\sim n+1}{\sigma^{a(j)}} = \left(1\text{-}\mathrm{D}^{(j)}_{n+1}\right)\ \underset{\sim n+1}{\sigma^{i}} + \mathrm{D}^{i}_{n+1}\ \sigma^{c}_{n+1} \qquad (25)$$

where *j* denotes iterations depicted in Fig. (15) (Desai, 2001b). Then the observed (applied) load is found as:

$$d\underset{\sim n+1}{\mathrm{Q}^{a}} = \int \underset{\sim}{\mathrm{B}^{T}}\ \underset{\sim n+1}{\sigma^{a(m)}}\ \mathrm{dV} \qquad (26)$$

where *m* denotes the last (converged) iteration.

5 VALIDATIONS

The DSC equations (1) are integrated to predict the observed laboratory behavior for a wide range of materials (Desai, 2001b). For most of the materials, the DSC model provides very good correlations with the test data for the *specimen level* tests. Also, the DSC model has provided very good correlations for independent test data, which were *not* used for calibration of the parameters. Details of validations at the practical *boundary problem level* are presented in a number of publications, e.g. Desai (2001b); three typical examples of applications are given below.

5.1 COMPUTER CODES

A computer code have been developed for (a) the determination of DSC parameters based on laboratory data. Here, the user can input points on various stress-strain-volumetric responses, and the code yields the parameters. This code also includes the integration of Eq. (1) by using the determined parameters so as to back predict stress-strain-volumetric responses toward validations at the specimen level.

Computer codes have been developed based on the above finite element method for static and dynamic analysis including liquefaction of practical boundary value problems, e.g. (i) DSC-SST2D (Desai 1999), (ii) DSC-DYN2D (Desai 2001c), and (iii) DSC-DYN3D (Desai 2001a). These and other codes have been used to solve a wide range of problems in civil, mechanical and electronic engineering. The predictions compare very

well with laboratory and/or field tests for practical problems. Three typical example problems for application of these codes are given below.

5.2 EXAMPLE 1: DYNAMIC BEHAVIOR OF PILE TESTED IN CENTRIFUGE

Fig. 16 shows the pile tested in the centrifuge test facility (Wilson, et al., 2000). The pile-Nevada sand system was subjected to base motion shown in Fig. 17. Various items such as pore water pressures, accelerations, displacements and bending moments were recorded with time by using instruments installed as marked in Fig. 16.

Finite element analysis was performed using a procedure based on generalized Biot's theory in which the DSC model was implemented (Desai, 2001c; Pradhan and Desai, 2006). The DSC model parameters for the Nevada sand were determined from laboratory triaxial tests reported by The Earth Technology Corporation for VELACS (Arulmoli, et al. 1992). The test data included three undrained monotonic triaxial tests and three undrained cyclic triaxial tests with continuing pressures, σ_3 = 40, 80 and 160 kPa at relative density, D_r = 60%. Details of the evaluation of parameters for the Nevada sand are given in Pradhan and Desai (2002); the values of the parameters are presented in Table 2.

The interface test data for the aluminum pile-Nevada sand were not available. Hence, a neural network approach was used for estimation of the parameter (Pradhan and Desai, 2002). Here, two sets of data for training of the neural network were used. Set 1 consisted of Ottawa sand parameters using triaxial tests (Park and Desai, 2000), and the Ottawa sand-steel interface using the cyclic multi-degree-of-freedom (CYMDOF) device (Alanazy, 1996 and Desai and Rigby, 1997). The second set consisted of parameters for a marine clay from triaxial and multiaxial testing (Katti and Desai, 1995) and marine clay-steel interface using the CYMDOF device (Shao and Desai, 2000). It was assumed that the steel and aluminum behave approximately similar in interfaces with the soil. Also, the Nevada sand gradation curve falls between those of the Ottawa sand and the marine clay. Finally, the parameters for Nevada sand-aluminum interface estimated from the neural network were found and are given in Table 2.

The sand and interface (aluminum-sand) were modeled using the DSC with the parameters given in Table 2. The aluminum pile itself was assumed to be linear elastic with elastic modulus = 70.0 GPa and Poisson's ratio = 0.33. The single pile, Fig. 16, was made of aluminum pipe with diameter of 0.67 m with wall thickness of 72 mm; the total depth of sand was 20.7 m and the embedment length of the pile was 16.8 m. The pile-system was idealized as plane strain (Pradhan and Desai, 2006; Anandarajah, 1992). The finite element mesh for the total domain in the centrifuge test for the pile is shown in Fig. 18(a); details of mesh around the pile are given in Fig. 18(b).

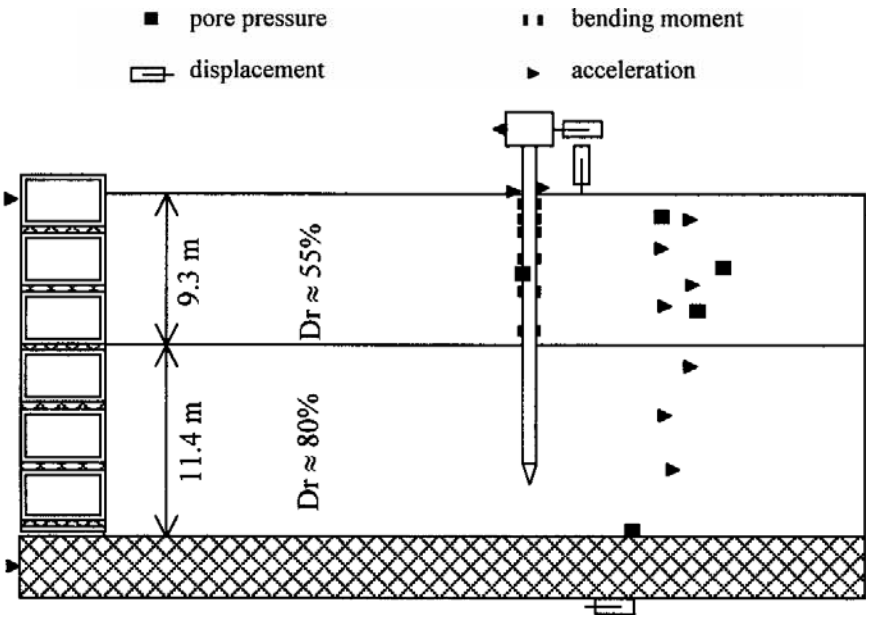

Figure 16. Schematic of pile in centrifuge test and instrumentation (from Wilson et al. 2000).

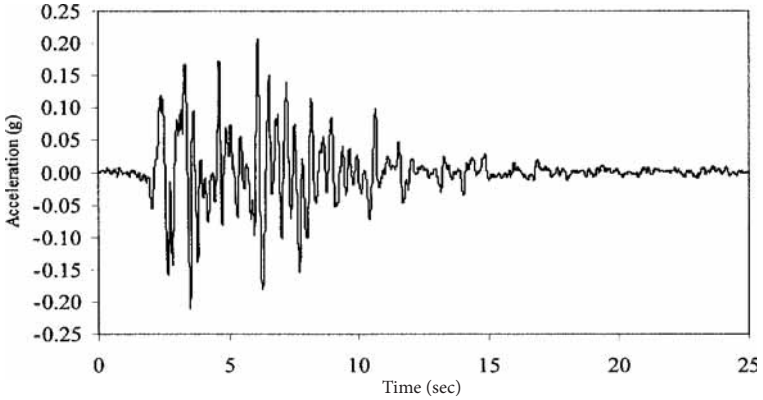

Figure 17. Base motion acceleration (from Wilson et al. 2000).

Table 2. Parameters for Nevada Sand and Sand-Aluminum Interface.

Material Parameter	Symbol	Nevada Sand	Nevada Sand - Aluminium Interface
RI: Elastic	E	41.0 MPa	14.6 MPa
	ν	0.316	0.384
RI: Plasticity	γ	0.0675	0.246
	β	0.00	0.00
	$3R$	0.00	0.00
	n	4.10	3.360
	a_1	0.1245	0.620
	η_1	0.0725	0.570
FA: Critical State	$\bar{m}$	0.22	0.304
	λ	0.02	0.0278
	e_o^c	0.712	0.791
Disturbance	D_u	0.99	0.990
	Z	0.411	1.195
	A	5.02	0.595

The FE mesh contained 302, 4-noded elements with 342 nodes. Interface elements were provided for the vicinity of pile by assuming small thickness of the sand. Boundary BC (Fig. 18a) was restrained in the y-direction, and AB and CD were free to move in both x- and y-directions. The base of mesh was subjected to the acceleration-time history shown in Fig. 17 (Wilson, et al., 2000).

The initial (in situ) and pore-water pressures at the centers of all elements were introduced by using:

$$\sigma_v' = \gamma_s h \; ; \; \sigma_{\mathrm{h}}' = K_o \; \sigma_{\mathrm{v}}' \; , \; \mathrm{K_o} = \nu/(1-\nu) \; , \text{ and } \mathrm{p} = \gamma_{\mathrm{w}} h \tag{27}$$

where σ_v' and σ_h' = effective vertical and horizontal stresses at depth, h; γ_s = submerged unit weight of soil; γ_w = unit weight of water; p = (initial) pore water pressure, and K_o = co-efficient of earth pressure at rest.

5.2 RESULTS

To identify the influence of interfaces between structure (pile) and soil, analyses were performed (a) without interfaces and (b) with interfaces. Only typical results are presented herein. Fig. 19 shows comparisons between measured pore water pressure in element 139 in the vicinity of the pile, and predictions with and without interface. The observed pore water pressure approaches the initial effective vertical pressure $\left(\sigma_v'\right)$, showing potential liquefaction, after about 9 seconds. The analysis without interface shows that the computed pore water pressure remains far from σ_v', i.e., it does not show liquefaction. However, the analysis with the interface shows that after about 9 seconds the pore water pressure is almost equal to σ_v', indicating liquefaction. Thus, provision of interface including related relative motions is considered to be essential for realistic prediction pore water pressures, liquefaction and behavior of the pile-soil system.

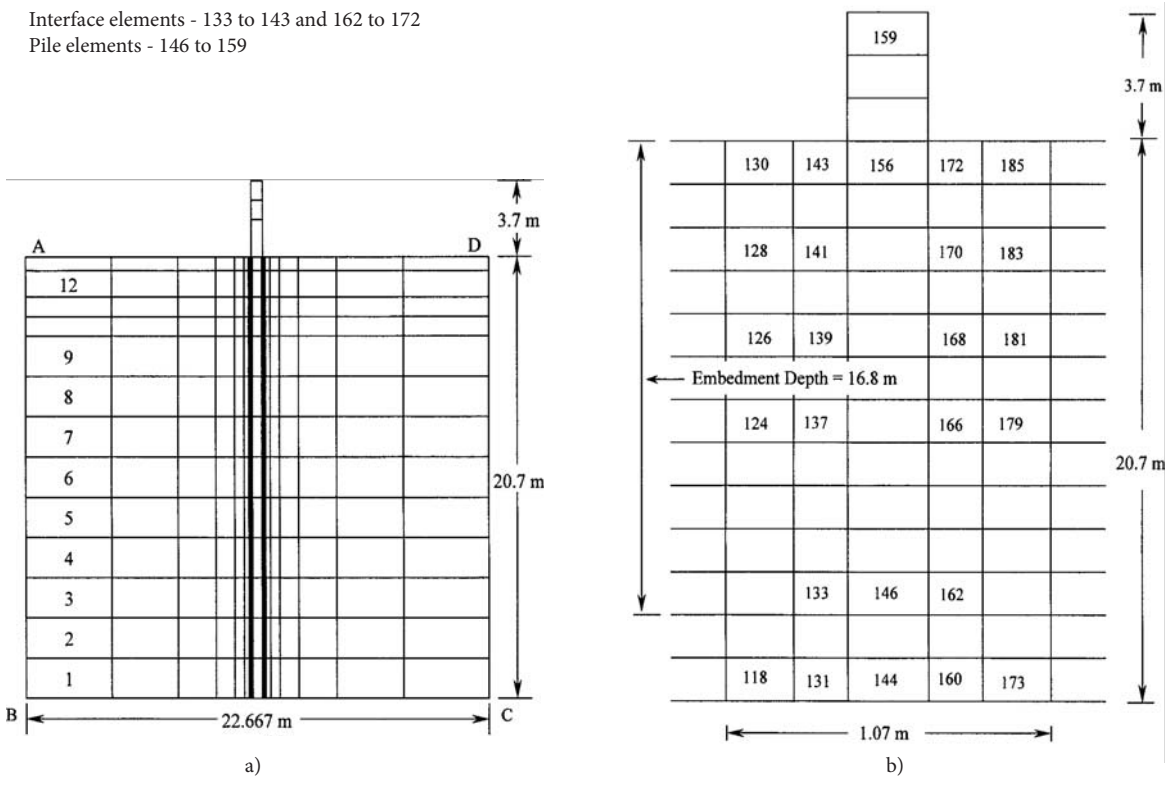

Figure 18. Finite element mesh for pile test.

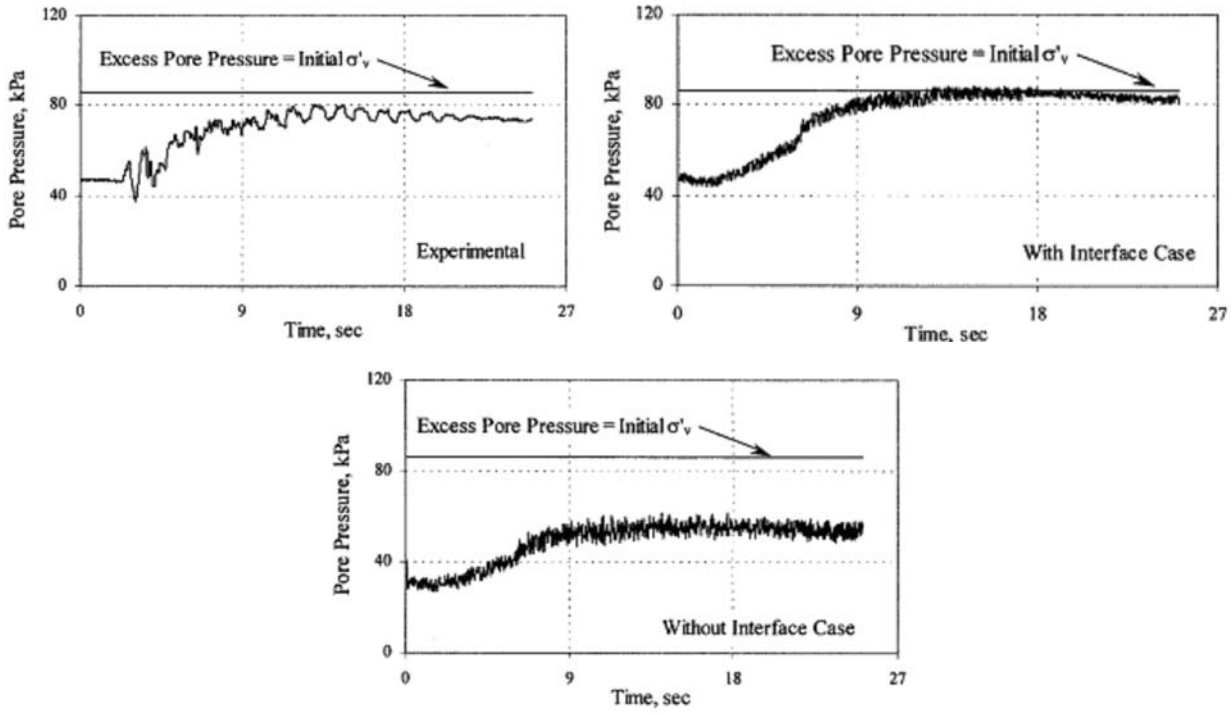

Figure 19. Comparisons of pore water pressures for element 139 in vicinity of pile.

Table 3 shows time to liquefaction in the conventional procedure when the pore water pressure, U_w, reaches the initial effective pressure $\sigma_v^{/}$. The time for reaching the critical disturbance, D_c = 0.86 (determined from the plot of disturbance vs. time), is considered to designate microstructural instability. Although the values of the two times are not too different, the times to reach D_c are lower than those to reach $\sigma_v^{/}$. This can imply that the microstructural instability may occur earlier than the time to liquefaction obtained from the conventional procedure. The conventional procedure suggests that the soil does not possess any strength when liquefaction occurs. In fact, it is observed that the soil can retain a small strength when the liquefaction is reached; this is also shown in observations during the Port Island, Kobe, Japan earthquake (Desai, 2000). Hence, it could be stated that the DSC based on the critical disturbance, D_c, could provide more accurate time to liquefaction (microstructural instability).

Table 3. Times to Liquefaction from Conventional and Disturbance Methods.

Element	Conventional $U_w = \sigma_v^{/}(s)$	Disturbance $D = D_c(s)$
143	1.74	1.23
130	1.83	1.29
104	2.55	1.92
78	3.36	2.67
52	3.81	2.94
26	9.03	8.22

5.3 EXAMPLE 2: REINFORCED EARTH RETAINING WALL

The DSC parameters for backfill (soil) and interface for a Tensar reinforced wall, Fig. 20 (USDOT 1989), were defined based on comprehensive laboratory tests, triaxial for soil, and interface shear for interfaces between soil and (Tensar) reinforcement (Desai and El Hoseiny, 2003). The DSC parameters for the backfill soil and interfaces are shown in Table 4.

The finite element procedure with the DSC model was used to analyze the earth retaining wall reinforced by using Tensar geogrid. Coarse and fine meshes were used for the analyses; it was found that the fine mesh analysis yields improved predictions compared to those from the coarse mesh. Fig. 21 shows a part of the fine mesh (with 11 layers); it contained 1188 nodes, and 1370 elements including 480 interface, 35 wall facings and 250 bar (reinforcement) elements.

The analysis included simulation of construction sequences, in which the backfill was constructed in 11 layers, as was done in the field. The reinforcement was placed on a layer after it was compacted. The completion of the sequences of construction is referred to as "end of construction." Then the surcharge load due to traffic of 20 kPa was added uniformly on the top of the mesh, which was referred to as "after opening to traffic." The *in situ* stress was introduced by using the co-efficient K_o = 0.40.

Table 4. Parameters to Analysis of Reinforced Wall.

Material Parameter	Symbol	Soil	Interface
RI: Elastic	E or k_n ν or k_s	$f_1(\sigma_3)^{a_1}$ 0.30	$f_2(\sigma_n)^b$ $f_3(\sigma_n)^c$
RI: Plasticity	γ β n a_1 η_1 k^d	0.12 0.45 2.56 3.0E^{-5} 0.98 0.20	2.30 0.00 2.80 0.03 1.00 0.40
Disturbance	D_u Z A	0.93 0.37 1.60	– – –
Angle of friciton and adhesion	$\phi/\delta/c_a$	ϕ = 40°	δ = 34° c_a = 66 kPa
Unit weight	$\bar{\gamma}$	18.00 kN/m^3	–
Co-efficient of earth pressure at rest	K_0	0.400	–

[a] $E = 62 \times 10^3\ \sigma_3^{0.28}$
[b] k_n (normal stiffness) $= 18 \times 10^3\ \sigma_n^{0.29}$
[c] k_s (shear stiffness) $= 30 \times 10^3\ \sigma_n^{0.28}$
[d] κ = nonassociative parameter

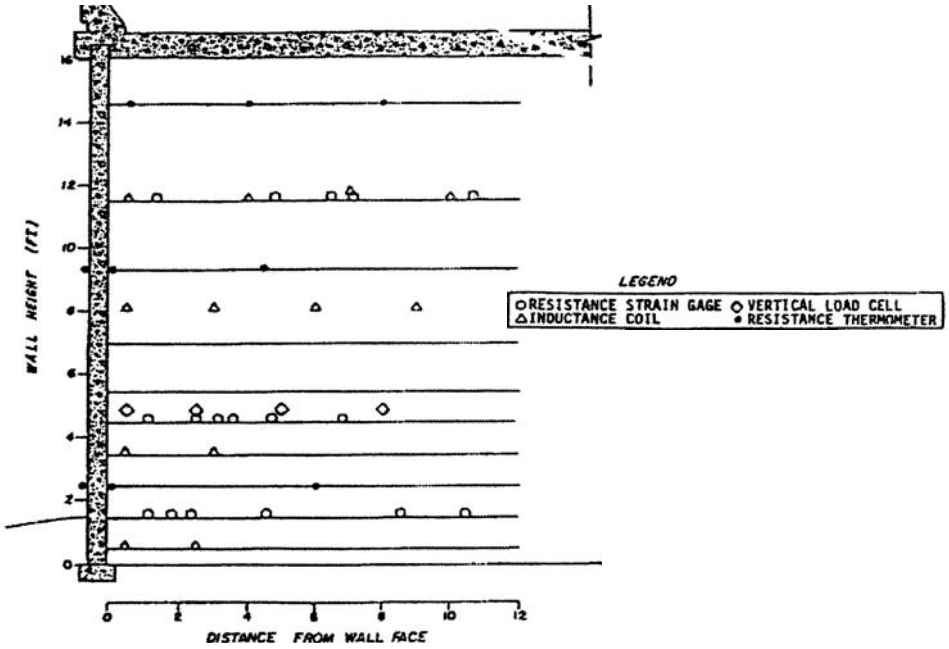

Figure 20. Tensar Reinforced wall (USDOT 1989).

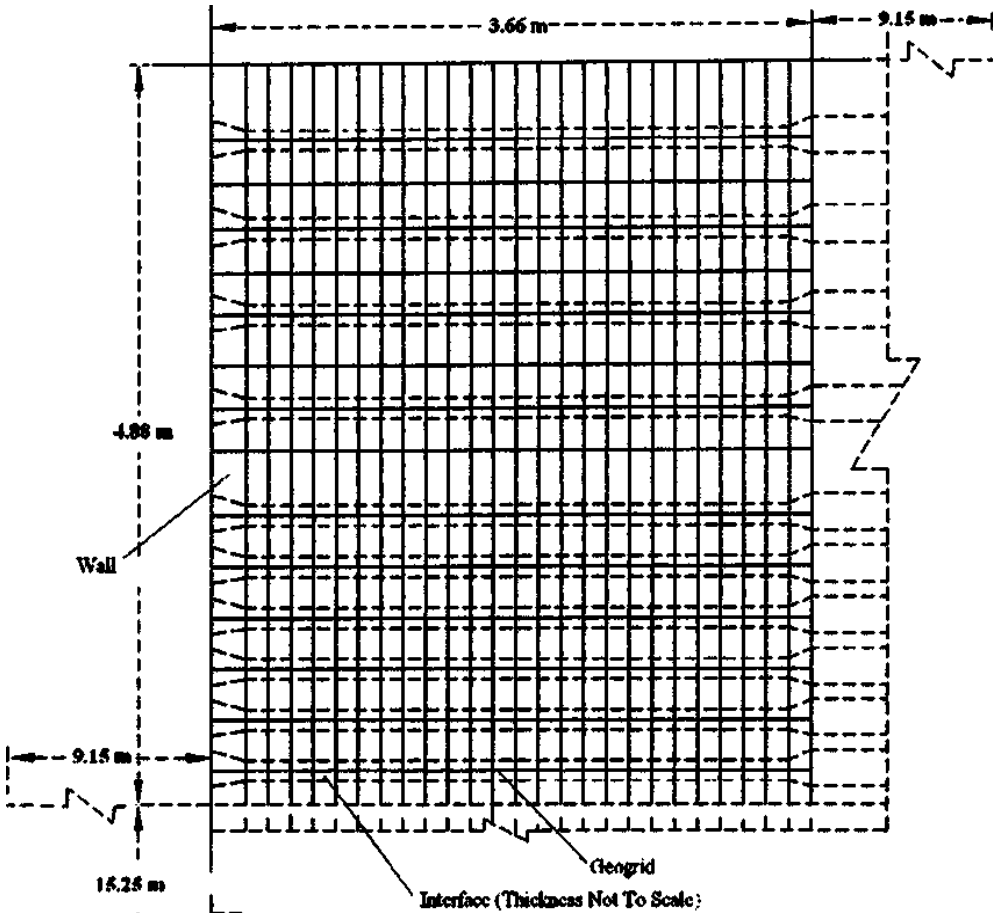

Figure 21. Fine Mesh (Part) for Tensar reinforced wall.

5.4 RESULTS

Only typical results are presented herein. Figure 22(a) shows comparison between predictions and field measurements for the vertical stress at elevation, 1.53 m, at the end of construction; those after opening to traffic are shown in Fig. 22(b). This figure shows also the overburden stress, and the trapezoidal vertical stress used in design calculations. The FE predictions agree well with the measured values.

Fig. 23 shows comparison between predictions and measurements for the horizontal stress carried by the geogrid near the wall face, at different elevations. The measurements are obtained from the strain gages installed on the geogrid. The predictions for the geogrid stresses compare well with the measurements.

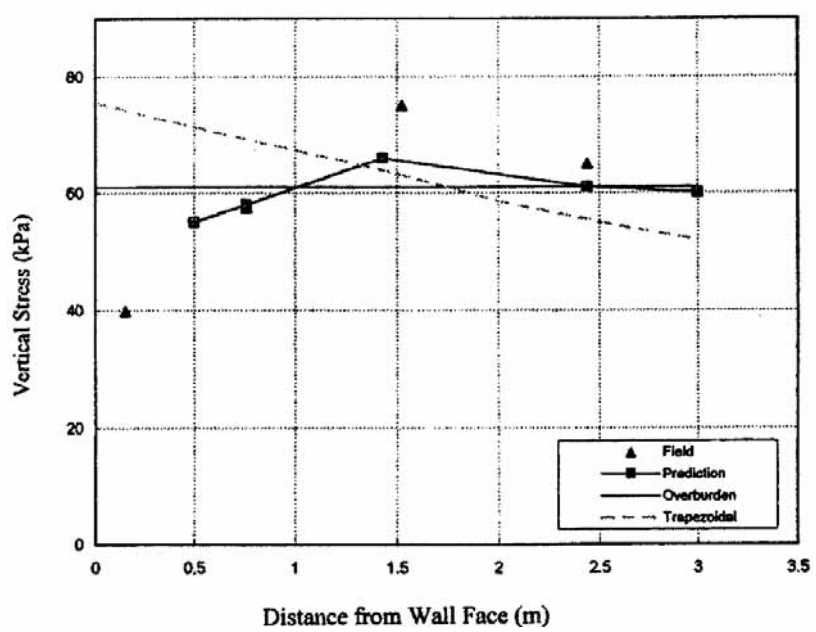

(a) End of construction

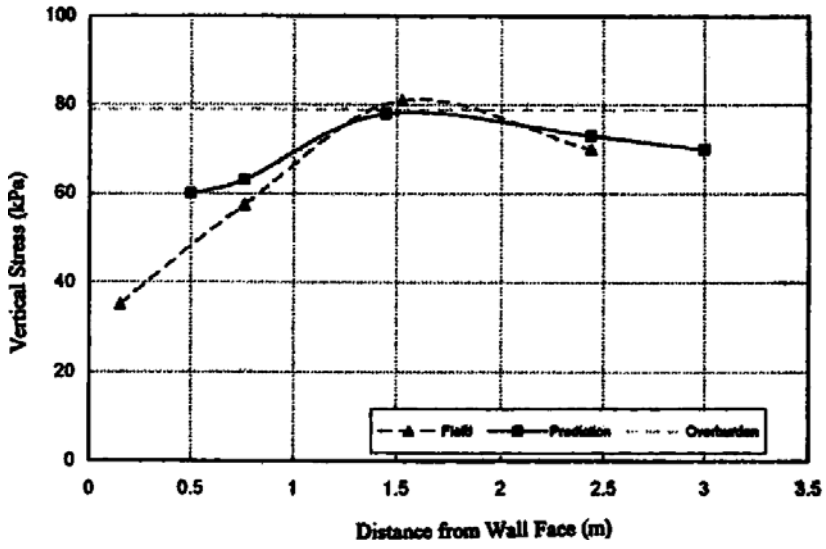

(b) After opening to traffic

Figure 22. Comparisons between field measurements and predictions for vertical stress at elevation 1.53 m.

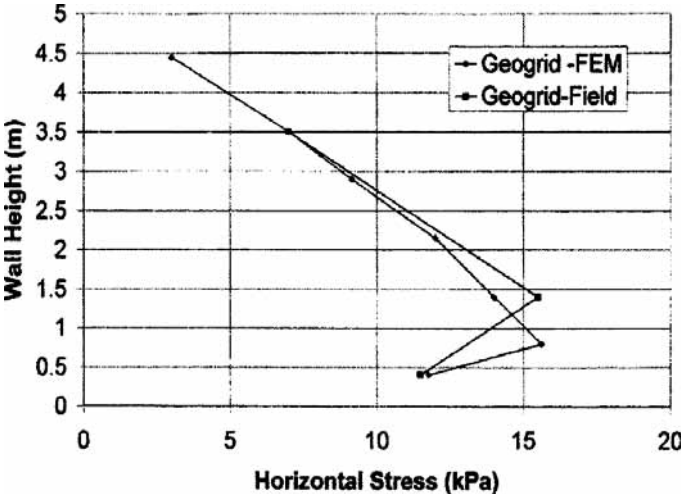

Figure 23. Comparison of field measurements and prediction for horizontal stress carried by geogrid near wall face.

5.5 EXAMPLE 3. MODELING FOR GLACIAL TILL FOR MOTION OF GLACIERS

Constitutive modeling of glacial till and till-ice interfaces play a significant role in predicting the movements of ice sheets or glaciers. The glacial till occurs between the ice and the base rock, and its deformations can contribute significantly to the motion of glaciers.

A comprehensive laboratory triaxial testing for shear and creep behavior of two glacial tills, Tiskilwa and Sky Pilot, were performed and used to define the DSC model (Desai et al., 2008, Sane, et al., 2008). The triaxial shear tests were performed under confining pressures, $\sigma_3^{/}$ = 20, 50, 100, 200, 300, 500 kPa. Tests were also performed for $\sigma_3^{/}$ = 150 and 400 kPa for independent validations of the model. Creep tests with constant (vertical) stress of 20, 40, 60 and 80% of the peak stress observed in the shear tests under $\sigma_3^{/}$ = 100, 200 and 400 kPa; tests under $\sigma_3^{/}$ = 300 kPa were performed for independent validation. These tests were used to find the parameters for the DSC model; Table 5 gives the parameters for two tills.

Note: Creep parameters for elastic-viscoplastic (evp) and viscoelastic-viscoplastic (vevp) models are given in Sane, et al. (2008).

The conventional plasticity models such as the Mohr-Coulomb have been used for behavior of glacial and till, and for identifications of the motion of glaciers. However, based on laboratory tests and finite element computations, it was found that the Mohr-Coulomb criterion that assumes failure and motion at maximum stress reached at very small (elastic) strains may not provide realistic behavior of till and initiation of motion.

Table 5. Parameters for Glacial Tills.

Material Parameter	Symbol	Tiskilwa Till	Sky Plot Till
RI: Elastic	E	57.75 MPa	50.50 MPa
	ν	0.45	0.45
RI: Plasticity	γ	0.0175	0.0092
	β	0.36	0.52
	n	3.60	6.85
	a_1	2.0 E^{-4}	1.35 E^{-7}
	η_1	0.27	0.14
FA: Critical State	$\bar{m}$	0.10	0.09
	λ	0.21	0.16
	e_o^c	0.48	0.52
Disturbance	D_u	1.00	1.00
	Z	2.68	1.00
	A	20.20	5.50

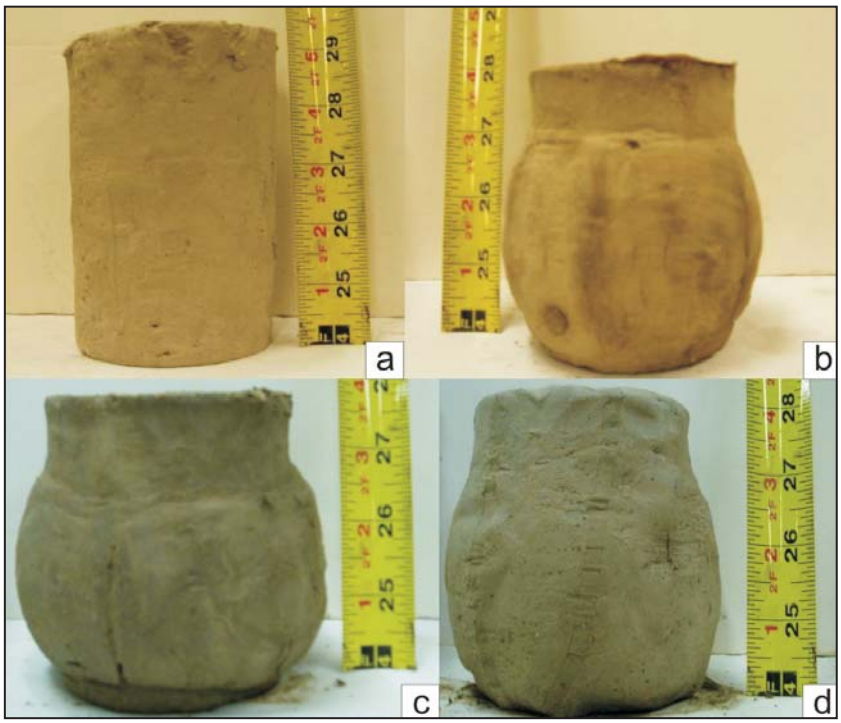

Figure 24. Photographs of triaxial test samples (a) before the test, and (b) after test for Sky Pilot till, and (c) and (d) after test,for Tiskilwa till.

It was observed that the glacial tills experience the disturbance at distributed locations in the test specimen, and fails when the critical disturbance, D_c, occurs in critical fraction of volume of the specimen. Fig. 24 shows the deformed configurations of till specimens which do not show specific failure planes, as is assumed in conventionally. In fact, it is considered that the "failure" in terms of the initiation of motion of the ice sheet may occur long after the peak stress, and at approximately the onset of the residual condition at D_c.

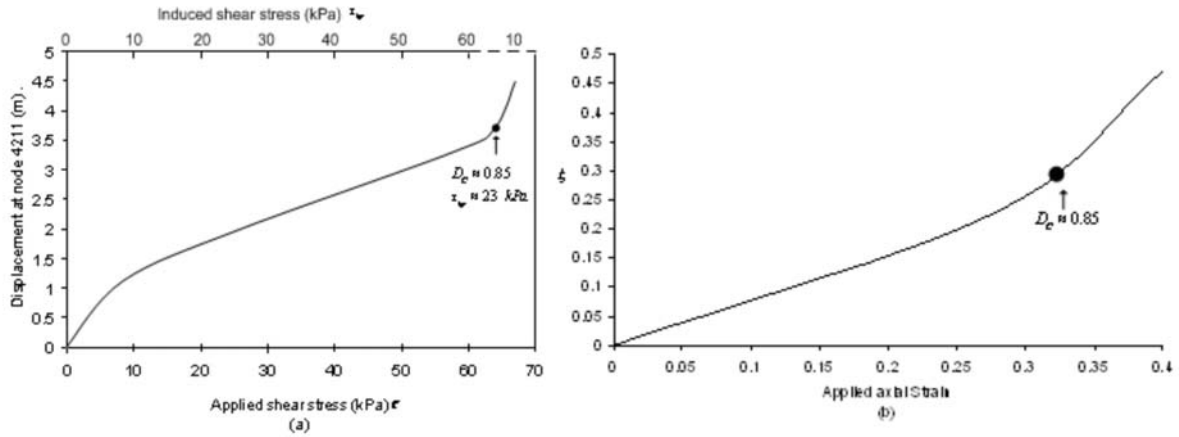

Figure 25. (a) Rate of change of displacement with applied stress predicted by finite element analysis, and (b) Rate of change of ξ with applied strain for triaxial test Tiskilwa till under confining stress = 100 kPa. Note: After the induced peak shear stress = 60 kPa, stress reduces to about 10 kPa in the post peak region, which is indicated by the dotted line in (a) above.

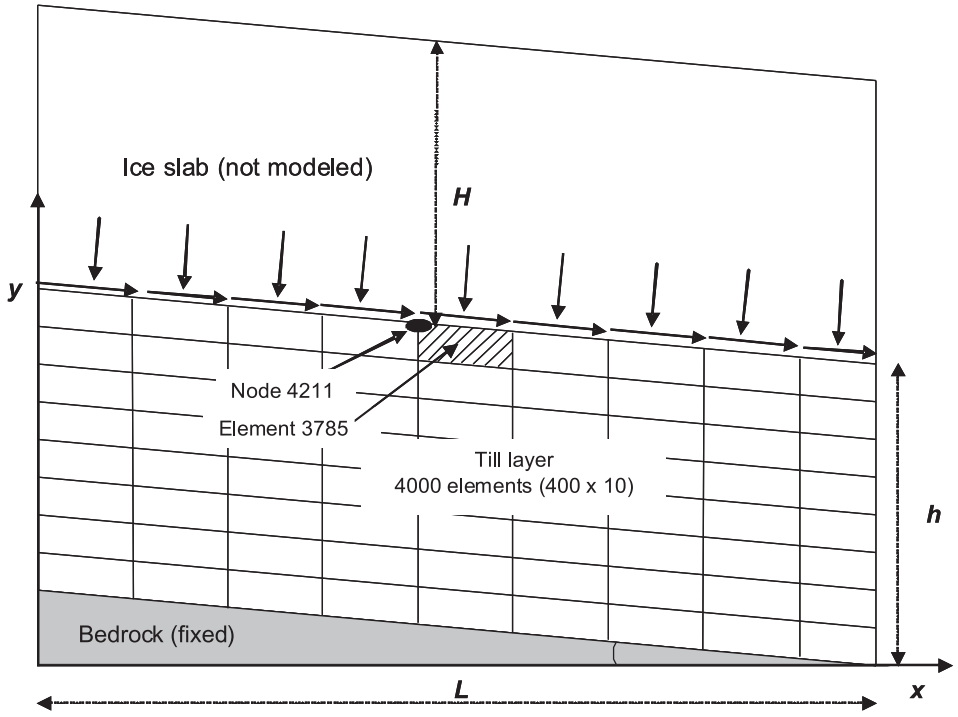

Figure 26. Simulated section of ice sheet on till and finite element mesh with loading. (Not to scale.)

Fig. 25(b) shows the plot of plastic strain trajectory (ξ) vs. applied axial strain for the behavior of the triaxial specimen under typical confining stress, σ_3' = 100 kPa. The instability causing failure or initiation of motion appears to occur when D_c = 0.85 is reached, which indicates the transition from linear to nonlinear behavior.

The above is also seen, Fig. 25(a), when the computed displacement vs. applied shear stress reaches D_c = 0.85 at the transition from linear to nonlinear behavior occurs. The results in Fig. 25(a) were obtained from the finite element analysis of a simulated problem involving ice sheets, till layer and bed rock, Fig. 26. The details of the finite element analysis are given in Sane, et al., 2008 and Desai, et al., 2008.

Thus, the DSC provides a realistic model for the behavior of glacial till and for the prediction of movements of ice sheets or glaciers, a subject which could have significant influence on global climate change.

6 CONCLUSIONS

Accurate modeling of the behavior of geologic materials and interfaces/joints are essential for realistic prediction of the behavior of geotechnical problems, e.g., by using computer (finite element) procedures. The disturbed state concept (DSC) provides unified and powerful constitutive models for solution of geotechnical and other engineering problems. This paper presents a description of the DSC including theoretical details, determination of parameters, and validations of the model at specimen level, and practical boundary value problem level. Typical examples of application of finite element procedures with the DSC model are presented and include comparisons between predictions with observations from field and laboratory simulated problems. The DSC model is considered to be unique and provides for successful modeling of a wide range of engineering materials, and interfaces and joints.

ACKNOWLEDGMENT

The results presented herein have been partly supported by a number of grants from the National Science Foundation, Washington, DC. Participation and contributions of a number of students and colleagues are acknowledged; some are included in the references.

REFERENCES

Alanazy, A.S. (1996). Testing and modeling of sand-steel interfaces under static and cyclic loading. *Ph.D. Dissertation*, Dept. of Civil Eng. and Eng. Mechanics, The University of Arizona, Tucson, AZ.

Anandarajah, A. (1992). Fully coupled analysis of a single pile foundation in liquefiable sands. *Report*, Dept. of Civil Eng., The Johns Hopkins University, Baltimore, Md.

Arulmoli, K., Muraleetharan, K.K., Hossain, M.M., and Fruth, L.S. (1992). VELACS: Verification of liquefaction analysis by centrifuge studies. *Soil Data Report*, The Earth Technology Corporation, Irvine, CA.

Baladi, G.Y., and Rohani, B. (1984). Development of an Elastic Viscoplastic constitutive relationship for earth materials. Chapter 2 in "Mechanics of Materials", Edited by Desai, C. S., and Gallagher, R.H., John Wiley and Sons Ltd, United Kingdom, 23-43.

Bazant, Z.P. (1994). Nonlocal damage theory based on micromechanics of crack interactions. *J. Eng. Mech., ASCE*, 120, 593-617.

Desai, C. S. (1974). A consistent finite element technique for work-softening behavior. *Proc., Int. Conf on Comp. Meth. in Nonlinear Mech*., J.T. Oden (editor), Univ. of Texas, Austin, TX, USA.

Desai, C.S. (1980). A general basis for yield, failure and potential functions in plasticity. *Int. J. Numer. Analy. Methods Geomech*., 4, 361-375.

Desai, C. S. (1987). Further on unified hierarchical models based on alternative correction or disturbance approach. Report, Dept. of Civil Eng. & Eng. Mech., The Univ. of Arizona, Tucson, AZ, USA.

Desai, C.S. (1999). DSC-SST2D-computer code for static, dynamic, creep and thermal analysis: Solid, structure and soil-structure problems. *Reports and Manuals*, Tucson, AZ, USA.

Desai, C.S. (2000). Evaluation of liquefaction using disturbed state and energy approaches. *J. of Geotech. and Geoenv. Eng., ASCE*, 126, 7, 618-631.

Desai, C.S. (2001a). DSC-SST3D-computer code for static and coupled dynamic analysis: Solid, (porous) structure and soil-structure problems. *Report and Manuals*, Tucson, AZ, USA.

Desai, C.S. (2001b). *Mechanics of Materials and Interfaces: The Disturbed State Concept*, CRC Press, Boca Raton, FL, USA..

Desai, C.S. (2001c). DSC-DYN2D-dynamic and static analysis, dry and coupled porous saturated materials. *Report and Manuals*, Tucson, AZ, USA.

Desai, C.S. (2007). Unified DSC constitutive model for pavement materials with numerical implementation. *Int. J. of Geomech*., 7, 2, 83-101.

Desai, C.S., Dishongh, T., and Deneke, P. (1998a). Disturbed state constitutive model for thermomechanical behavior of dislocated silicon with impurities. *J. of Applied Physics*, 84, 11, 5977-5984.

Desai, C.S., and El-Hoseiny, K.E. (2005). Prediction of field behavior of reinforced soil wall using advanced constitutive model. *J. of Geotech. and Geoenviron. Eng., ASCE*, 131, 6, 729-739.

Desai, C.S., and Ma. Y. (1992). Modelling of joints and interfaces using the disturbed state concept. *Int. J. Num. and Analyt. Methods in Geomech*., 16, 9, 623-653.

Desai, C.S., Park, I.J., and Shao, C. (1998b). Fundamental yet simplified model for liquefaction instability. *Int. J. Num. Analyt. Meth. in Geomech*., 22, 7, 721-748.

Desai, C.S., Pradhan, S.K., and Cohen, David (2005). Cyclic testing and constitutive modeling of saturated sand-concrete interfaces using the Disturbed State Concept. *Int. J. of Geomechanics*, 5, 4, 286-294.

Desai, C.S., and Rigby, D.B. (1997). Cyclic interface and joint shear device including pore pressure effects. *J. of Geotech. and Geoenviron. Eng*., 123, 6, 568-579.

Desai, C.S., Sane, S.M., and Jenson, J.W. (2008). Constitutive modeling and testing of glacial tills for prediction of motion of glaciers. *Proc., Int. conf. on Conf. Methods and Advances in Geomech*., Goa, India, 4494-4508.

Desai, C.S., Samtani, N.C., and Vulliet, L. (1995). Constitutive modeling and analysis of creeping slopes. *J. Geotech. Eng*., ASCE, 121, 43-56.

Desai, C.S., Somasundaram, S., and Frantziskonis, G. (1986). A hierarchical approach for constitutive modeling of geologic materials. *Int. J. Numer. Anal. Methods in Geomech*., 10, 3, 225-257.

Desai, C.S., and Toth, J. (1996). Disturbed state constitutive modeling based on stress-strain and nondestructive behavior. *Int. J. Solids & Struct*., 33, 11, 1619-1650.

Desai, C.S., and Whitenack, R. (2001). Review of models and the disturbed state concept for thermo -mechanical analysis in electronic packaging. *J. Electron. Packaging*, 123, 1-15.

Desai, C.S., Zaman, M.M., Lightner, J.G., and Siriwardane, H.J.(1984). Thin-layer element for interfaces and joints. *Int. J. Num. and Analyt. Methods in Geomech*., 8,1, 19-43.

Duwez, P. (1935). On plasticity of crystals. *Physical Reviews*, 47, 6, 494-501.

Elgamal, A., Yang, Z., and Parra, E. (2002). Computational modeling of cyclic mobilityand post-liquefaction site response. *Soil Dynamics and Earthquake Eng*., 22, 259-271.

Geiser, F., Laloui, L., Vulliet, L., and Desai, C.S. (1997). Disturbed state concept for partially saturated soils. *Proc., 6th Intl. Symp. on Num. Models in Geomechanics*, Montreal, Pietrusczka, S. and Pande, G.N. (Eds.), Canada, Balkema, Netherlands.

Huang, Y.H. (1993). Pavement Analysis and Design, Prentice-Hall, Englewood Cliffs, NJ.

Kachanov, L.M. (1986). *Introduction to Continuum Damage Mechanics*, Martinus Nijhoff Publishers, Dordrecht, The Netherlands.

Katti, D.R., and Desai, C.S. (1995). Modeling and testing of cohesive soil using the disturbed state concept. *J. of Eng. Mech*., ASCE, 121, 5, 648-658.

Lade, P.V., and Kim, M.K. (1988). Single hardening constitutive model for frictional materials. III. Comparisons with experimental data. *Computers and Geotechnics*, 6, 31-47.

Matsuoka, H., and Nakai, T. (1974). Stress-deformation and strength characteristics of soil under three different principal stresses. *Proc., Jap. Soc. Civil Engrs*., 232, 59-70.

Mroz, Z., Norris, V.A., and Zienkiewicz, O.C. (1978). An anisotropic hardening model for soils and its application to cyclic loading. *Int. J. Num. & Analyt. Methods in Geomech*., 2, 208-221.

Mühlhaus, H.B. (Ed.) (1995). *Continuum Models for Materials with Microstructure*, John Wiley, UK.

Pande, G.N., Owen , D.R.J., and Zienkiewicz, O.C. Overlay models in time dependent nonlinear material analysis," *Computers and Structures*, 7, 435-443.

Park, I.J., and Desai, C.S. (2000). Cyclic behavior and liquefaction of sand using disturbed state concept. *J. Geotech. Geoenv. Eng*., ASCE, 126, 9.

Perzyna, P. (1966). Fundamental problems in viscoplasticity. *Adv. in Appl. Mech*., 9, 243-277.

Pestana, J.M., and Whittle, A.J. (1999). Formulation of a unified constitutive model for clays and sands. *Int. J. Num. & Analyt. Methods in Geomech*., 23 (12), 1215-1243.

Pradhan, S.K., and Desai, C.S. (2002). Dynamic soil-structure interaction using disturbed state concept and artificial neural networks for parameter evaluation. *NSF Report*, Dept. of Civil Eng. and Eng. Mechanics, The University of Arizona, Tucson, AZ.

Pradhan, S.K., and Desai, C.S. (2006). DSC model for soil and interface including liquefaction and prediction of centrifuge test. *J. of Geotech. and Geoenviron. Eng*., ASCE, 132, 2, 214-222.

Roscoe, A.N., Schofield, A., and Wroth, P.C. (1958). On yielding of soils. *Geotechnique*, 8, 22-53.

Sane, S.M., Desai, C.S., and Rassaian, M. (2009). Rate dependent constitutive modeling of lead free solders in electronic packaging. Journal of Electronic Packaging, ASME, submitted.

Sane, S.M., Desai, C.S., Jenson, J.W., Contractor, D.N., Carlson, A.E., and Clark, P.U. (2008). Disturbed state constitutive modeling of two Pleistocene tills. *Quaternary Science Reviews*, 27, 267-283.

Shao, C., and Desai, C.S. (2000). Implementation of DSC model and application for analysis of field pile tests under cyclic loading. *Int. J. Num. Analyt. Meth. Geomech*., 24, 6, 601-624.

Somasundaram, S., and Desai, C.S. (1988). Modelling and testing for anisotropic behavior of soils. *J. Eng. Mech*., ASCE, 114, 1473-1496.

Šuklje, L. (1969). Rheological aspects of soil mechanics. Wiley-Interscience, London.

United States Department of Transportation (USDOT) (1989). Tensar geogrid reinforced soil wall. Experimental Project 1, Ground modification techniques", FHWA-EP-90-001-005, Washington, D.C.,

Wathugala, G.W., and Desai, C.S. (1993). Constitutive model for cyclic behavior of clays-theory, Part I. *J. of Geotech. Eng*., 119, 4, 714-729.

Wilson, D.N., Boulanger, R.W., and Kutter, B.L. (2000). Observed seismic lateral resistance of liquefying sand. *J. Geotech. Geoenviron. Eng*., ASCE, 126, 10, 898-906.

Zienkiewicz, O.C., Nayak, G.C., and Owen, D.R.J. (1972). Composites and overlay models in numerical analysis of elasto-plastic continua. *Proc. Int. Symp. On Foundations of plasticity*, Warsaw, Poland.